Adv Polym Sci
DOI: 10.1007/12_2013_258

Computational Studies of Biomembrane Systems: Theoretical Considerations, Simulation Models, and Applications

Markus Deserno, Kurt Kremer, Harald Paulsen, Christine Peter, and Friederike Schmid

Abstract This chapter summarizes several approaches combining theory, simulation, and experiment that aim for a better understanding of phenomena in lipid bilayers and membrane protein systems, covering topics such as lipid rafts, membrane-mediated interactions, attraction between transmembrane proteins, and aggregation in biomembranes leading to large superstructures such as the light-harvesting complex of green plants. After a general overview of theoretical considerations and continuum theory of lipid membranes we introduce different options for simulations of biomembrane systems, addressing questions such as: What can be learned from generic models? When is it expedient to go beyond them? And, what are the merits and challenges for systematic coarse graining and quasi-atomistic coarse-grained models that ensure a certain chemical specificity?

M. Deserno (✉)
Department of Physics, Carnegie Mellon University, 5000 Forbes Ave., Pittsburgh, PA 15213, USA
e mail: deserno@andrew.cmu.edu

K. Kremer
Max Planck Institute for Polymer Research, Ackermannweg 10, 55128 Mainz, Germany
e mail: kremer@mpip mainz.mpg.de

H. Paulsen
Department of Biology, University of Mainz, Johannes von Müller Weg 6, 55128 Mainz, Germany
e mail: paulsen@uni mainz.de

C. Peter
Department of Chemisty, University of Konstanz, Universitätsstraße 10, 78457 Constance, Germany
e mail: christine.peter@uni konstanz.de

F. Schmid
Institute of Physics, University of Mainz, Staudingerweg 9, 55128 Mainz, Germany
e mail: schmid@uni mainz.de

Keywords Coarse graining · Curvature elasticity · Lipid bilayer · Mediated interactions · Multiscaling · Simulation

Contents

1 Introduction

Lipid bilayers and membrane proteins are one important class of biological systems for which the relationship between single molecule properties and the behavior of complex nanoscopically structured materials has been under intense investigation for a long time. In the present review we address how approaches combining theory, simulation, and experiment may help us gain a better understanding of phenomena in biomembranes. A general overview of theoretical considerations and continuum theory of lipid membranes is given and different modeling and simulation approaches to biomembrane systems are introduced. In particular, we introduce several generic lipid simulation models and show how these models can help us understand material properties of lipid bilayers such as bending and Gaussian curvature modulus, or membrane tension. We discuss timely topics such as lipid rafts, membrane protein interactions, and curvature-mediated interactions between proteins. These fundamental theoretical and modeling investigations are important for understanding the principles that govern the aggregation phenomena in biological membranes that lead to large superstructures such as the light-harvesting complex of green plants. In Sect. 4 of this chapter, we give an overview of multiscale modeling approaches that try to go beyond generic lipid and protein models and attempt to ensure a certain chemical specificity while still benefiting from the time- and length-scale advantages of coarse-grained simulations. The section concludes with the example of the light-harvesting complex of green plants, for which we show first steps toward a multiscale simulation model that allows one to go back and forth between a coarse-grained and an atomistic

level of resolution and therefore permits immediate comparison with atomic level experimental data.

2 Theory and Simulation of Lipid Bilayers

To provide a basis for both the theoretical ideas and the computational techniques that we will discuss in this chapter, we start by reminding the reader of some essential concepts. Section 2.1 reviews some basic aspects of the Helfrich Hamiltonian. Section 2.2 introduces three coarse-grained membrane models that will be used in the remainder of this chapter. In Sects. 2.3 and 2.4, we discuss the bending moduli and the surface tension of membranes in more detail, and finally comment on multicomponent membranes in Sect. 2.5.

2.1 Basic Continuum Theory Concepts

2.1.1 Continuum Elasticity of Lipid Membranes

Lipid molecules are amphipathic: they consist of a hydrophilic head group and typically two hydrophobic (fatty acid) tails. Yet, despite their amphipathic nature, lipid molecules dissolved in water have an extremely low critical aggregate concentration (nanomolar or even smaller [1]), and thus under most common conditions lipids spontaneously aggregate. Because the roughly cylindrical shape of lipids leads to two-dimensional self-assembly, thermodynamic considerations [2] show that in contrast to the finite size of spherical and wormlike micelles a single macroscopic aggregate containing almost all of the lipids will form: a two-dimensional bilayer membrane. Its lateral dimensions can exceed its thickness by several orders of magnitude.

2.1.2 The Helfrich Hamiltonian

If lipid membranes are subjected to lateral tension, they typically rupture at stresses of several millinewtons per meter (mN/m), with a remarkably low rupture strain of only a few percent [3]. At large scales and moderate tensions it is hence an excellent approximation to consider membranes as largely unstretchable two-dimensional surfaces. Their dominant soft modes are not associated with stretching but with bending [4–6]. Within the well-established mathematical framework developed by Helfrich [5], the energy of a membrane patch $\mathcal{P}$, amended by a contribution due to its boundary $\partial\mathcal{P}$ [7], is expressible as:

$$E[\mathscr{P}] = \int_{\mathscr{P}} \mathrm{d}A \left\{ \frac{1}{2}\kappa(K - K_0)^2 + \overline{\kappa} K_\mathrm{G} \right\} + \oint_{\partial\mathscr{P}} \gamma. \tag{1}$$

Here, $K = c_1 + c_2$ and $K_\mathrm{G} = c_1\, c_2$ are the total and Gaussian curvature, respectively, and the c_i are the local principal curvatures of the surface [8, 9]. The inverse length K_0 is the spontaneous bilayer curvature, showing that the first term quadratically penalizes the deviation between total and spontaneous curvature.[1] The parameters κ and $\overline{\kappa}$ are the bending modulus and Gaussian curvature modulus, respectively, and they quantify the energy penalty due to bending. Finally, the parameter γ is the free energy of an open membrane edge and is thus referred to as the edge tension.

2.1.3 Refining the Helfrich Model

Although the Helfrich Hamiltonian provides a successful framework for describing the large-scale structure and geometry of fluid membranes, it is not designed for modeling membranes on smaller length scales, i.e., of the order of the membrane thickness. Several more refined continuum models have been proposed for amending this situation. Evidently, continuum descriptions are no longer applicable at the Ångström scale. However, they still turn out to be quite useful on length scales down to a few nanometers.

As one refinement, Lipowsky and coworkers have proposed the introduction of a separate, independent "protrusion" field that accounts for short wavelength fluctuations [10 12]. According to recent atomistic and coarse-grained simulations by Brandt et al., these protrusions seem to correspond to lipid density fluctuations within the membrane [13, 14]. Lindahl and Edholm pioneered another important refinement, which is to consider the height and thickness variations of membranes separately [15]. Continuum models for membranes with spatially varying thickness have a long-standing tradition in theories for membrane-mediated interactions between inclusions [16 27] (see also Sect. 3.1), and they can be coupled to Helfrich models for height fluctuations in a relatively straightforward manner [28 30]. In addition, one can include other internal degrees of freedom, such as local tilt [31 36], as well as membrane tension [36, 37].

In this article, we will focus in particular on the so-called coupled monolayer models [18, 20 26, 28, 29], where membranes are described as stacks of two sheets (monolayers), each with their own elastic parameters. Monolayers are bound to each other by a local harmonic potential that accounts for the areal compressibility of lipids within the membrane and their constant volume [22, 28]. Li et al. have recently compared the elastic properties of amphiphilic bilayers with those of the corresponding monolayers within a numerical self-consistent field study of

[1] Observe that $1/K_0$ is not the optimal radius R_opt of a spherical vesicle. Minimizing the energy per area with respect to K shows that instead this radius is given by $R_\mathrm{opt}K_0 \quad 2 + \overline{\kappa}/\kappa$.

copolymeric membranes [38]. They found that the bilayer elastic parameters can be described at an almost quantitative level by an appropriate combination of monolayer elastic parameters.

2.2 Coarse-Grained Lipid Models

The multitude of length and time scales that matter for biophysical membrane processes is mirrored in a wide spectrum of computational models that have been devised to capture these scales. These range from all-atom simulations [39 43] up to dynamically triangulated surfaces [44 47] and continuum models [48, 49]. The region in between is becoming increasingly populated by a wealth of different coarse-grained (commonly abbreviated "CG") models, which capture different aspects of a very complex physical situation, and a number of excellent reviews exist that provide a guide to the literature [50 57].

Besides their chosen level of resolution, CG models can also be classified by the "spirit" in which they approach a physical situation: If the focus lies on generic mechanisms that are thought to be quite universal in their reach, there is no need to construct models that faithfully relate to every aspect of some particular lipid. Instead, one creates "top-down" models based on the presumed principles underlying the generic mechanisms of interest. For instance, if one wishes to understand how a bilayer membrane interacts with a colloidal particle that is much bigger than the thickness of the membrane, relevant aspects of the situation will likely include the fluid curvature elastic response of bilayer lipid membranes, but probably not the hydrogen bonding abilities of a phosphatidylethanol head group. If, in contrast, one wishes to understand how mesoscopic membrane properties emerge from specific properties of their microscopic constituents, the aim is instead to construct "bottom-up" models whose key design parameters follow in a systematic way from those of a more finely resolved model. For instance, if one wishes to understand how those hydrogen bonding abilities of a phosphatidylethanol head group impact the mesoscopic phase behavior of mixed bilayers, it will not do to simply guess a convenient head group interaction potential, even if it is eminently plausible. The latter philosophy goes under various names, such as "systematic coarse graining" or "multiscaling" and again excellent literature and resources exist that cover this field [58 72].

The top-down and bottom-up approaches are not necessarily mutually exclusive. It is conceivable that certain aspects of the science are systematically matched, while others are accounted for in a generic way by using intuition from physics, chemistry, mathematics, or other pertinent background knowledge. Conversely, this also means that what any given model can qualitatively or quantitatively predict depends greatly on the way in which it has been designed; there is no universally applicable CG model. Stated differently, systematically coarse-grained models will not be accurate in every prediction they make, and generic models can

be highly quantitative and experimentally testable. One always needs to know what went into a given model to be able to judge the reliability of its predictions.

In Sects. 2.2.1 2.2.3, we will review the basics of three particular CG models that will feature in the remainder of this paper. The choice of models is not meant to imply a quality statement but merely reflects our own experience and work.

2.2.1 Cooke Model

The Cooke model [73, 74] is a strongly coarse-grained top-down lipid model in which every single lipid is represented by three linearly connected beads (one for the head group, two for the tail) and solvent is implicitly accounted for through effective interactions. It is purely based on pair interactions and therefore very easy to handle. Its main tuning parameters are the temperature and the range w_c of the effective cohesion that drives the aggregation of the hydrophobic tail beads. One might also change the relative size between head and tail beads to control the lipids' spontaneous curvature [75]. The bead size σ serves as the unit of length and the potential depth ϵ as the unit of energy. For the common choice $k_BT/\epsilon = 1.1$ and $w_c/\sigma = 1.6$, lipids spontaneously assemble into fluid membranes with an area per lipid of about 1.2 σ^2, a bending rigidity of $\kappa \approx 12.8\ k_BT$ (but rigidities between 3 k_BT and 30 k_BT can be achieved without difficulty), and an elastic ratio of $\overline{\kappa}/\kappa \approx -0.92$ [76].

2.2.2 Lenz Model

Like the Cooke model, the Lenz model [77] is a generic model for membranes, but it has been designed for studying internal phase transitions. Therefore, it puts a slightly higher emphasis on conformational degrees of freedom than the Cooke model. Lipids are represented by semiflexible linear chains of seven beads (one for the head group, six for the tail), which interact with truncated Lennard Jones potentials. Model parameters such as the chain stiffness are inspired by the properties of hydrocarbon tails [78]. The model includes an explicit solvent, which is, however, modeled such that it is simulated very efficiently: it interacts only with lipid beads and not with itself ("phantom solvent" [79]).

The model reproduces the most prominent phase transitions of phospholipid monolayers [78] and bilayers [80]. In particular, it reproduces a main transition from a fluid membrane phase (L_α) to a tilted gel phase ($L_{\beta'}$) with an intermediate ripple phase ($P_{\beta'}$), in agreement with experiments. The elastic parameters have been studied in the fluid phase and are in reasonable agreement with those of saturated DPPC (dipalmitoyl-phosphatidylcholine) bilayers. Recently, the Lenz model has been supplemented with a simple cholesterol model [81]. Cholesterol molecules are taken to be shorter and stiffer than lipids, and they have a slight affinity to lipids. Mixtures of lipids and cholesterol were found to develop nanoscale raft domains

[81], in agreement with the so-called "raft hypothesis" [82]. As a generic model that reproduces nanoscale structures in lipid membranes (ripple states and rafts), simulations of the Lenz model can provide insight into the physics of nanostructure formation in lipid bilayers. This will be discussed in more detail in Sect. 2.5.

2.2.3 MARTINI Model

The MARTINI model for lipids [83, 84] is a hybrid between a top-down and a bottom-up model: approximately four heavy atoms are mapped to a single CG bead, and these CG beads come in a variety of types, depending on their polarity, net charge, and the ability to form hydrogen bonds. The systematic aspect of MARTINI largely derives from the fact that the nonbonded interactions between these building blocks (shifted Lennard Jones and possibly shifted Coulomb potentials) have been parameterized to reproduced most of the thermodynamics correctly, especially the partitioning free energy between different environments, such as between aqueous solution and oil. Given a particular molecule, a judicious choice of assignments from groups of heavy atoms to MARTINI beads, together with standard bonded interactions (harmonic, angular, and dihedral potentials), leads to the CG version of a molecule.

The complete MARTINI force field encompasses more than lipids and sterols [83, 84]; it is currently also available for proteins [85], carbohydrates [86], and glycolipids [87]. The far-reaching possibilities for looking at multicomponent systems without the need to explicitly cross-parametrize new interactions have substantially contributed to the attractiveness of this force field. Of course, care must still be taken that one's mapping onto the CG level is consistent overall and chemically meaningful: Even though the nonbonded interactions are derived from a single guiding principle, which is both conceptually attractive and computationally powerful, there is no guarantee that it will work under all circumstances for one's particular choice of system and observable, so it is up to the user to perform judicious sanity checks. After all, with great power there must also come great responsibility [88].

2.3 Obtaining Material Parameters

The Hamiltonian in Eq. (1) is an excellent phenomenological description of fluid membranes, but it does not predict the material parameters entering it, which must instead come from experiment or simulation. Let us briefly list a number of ways in which this is achieved, both in experiment and in simulation.

The bending modulus κ is measured by techniques such as monitoring the thermal undulations of membranes [89 94], probing the low-tension stress strain relation [95], X-ray scattering [96 99], neutron spin echo measurements [100 102] (note however the caveats raised by Watson and Brown [103]), or pulling thin

membrane tethers [104–106]. In simulations, monitoring undulations [12, 15, 28, 73, 74, 83, 107–111] or orientation fluctuations [112], measuring tensile forces in tethers [111, 113, 114], and buckling [115, 116] have been used successfully.

The Gaussian curvature modulus $\overline{\kappa}$ is much harder to obtain because, by virtue of the Gauss-Bonnet theorem [8, 9], the surface integral over the Gaussian curvature K_G depends only on the topology and the boundary of the membrane patch $\mathcal{P}$. Hence, one needs to change at least one of them to access the Gaussian curvature modulus. It therefore tends to be measured by looking at the transitions between topologically different membrane phases (e.g., the lamellar phase L_α and the inverted cubic phase Q_{II}) [117–120] or the shape of phase-separated membranes in the vicinity of the contact line [121, 122] (even though the latter strictly speaking only gives access to the difference in Gaussian moduli between the two phases). In Sect. 2.3.2 we will briefly present a computational method that obtains $\overline{\kappa}$ from the closure probability of finite membrane patches [76, 123].

To measure the edge tension requires an open edge, and in experiments this essentially means looking at pores [124–127]. This also works in simulations [73, 74, 83, 108, 109], but it tends to be easier to create straight bilayer edges by spanning a "half-membrane" across the periodic boundary conditions of the simulation box [128–131].

The spontaneous curvature K_0 usually vanishes due to bilayer up–down symmetry, but could be measured by creating regions of opposing spontaneous curvature and monitoring the curvature this imprints on the membrane [132], or by measuring the shape of a spontaneously curved membrane strip [111].

Because curvature elasticity is such an important characteristic of lipid membranes, obtaining the associated moduli has always attracted a lot of attention. Let us therefore provide a few more details on some classical and some more recent computational strategies to measure them. Shiba and Noguchi [111] also provide a detailed recent review.

2.3.1 Bending Modulus

The shape of essentially flat membranes stretched across the periodic boundary conditions of a simulation box can be described by specifying their vertical displacement $h(\boldsymbol{r})$ above some horizontal reference plane, say of size $L \times L$. In this so-called Monge parametrization, the bending contribution due to the total curvature term (ignoring for now on the spontaneous curvature K_0) is given by:

$$\int \mathrm{d}A \frac{1}{2}\kappa K^2 = \frac{1}{2}\kappa \int_{[0,L]^2} \mathrm{d}^2 r \ \sqrt{1+(\nabla h)^2} \left(\nabla \cdot \frac{\nabla h}{\sqrt{1+(\nabla h)^2}} \right)^2 \qquad (2)$$

$$= \frac{1}{2}\kappa \int_{[0,L]^2} \mathrm{d}^2 r \; \left\{ (h_{ii})^2 - \frac{1}{2}(h_{ii})^2 h_j h_j - 2h_{ii} h_j h_{jk} h_k + \mathcal{O}\left(h^6\right) \right\}, \tag{3}$$

where the indices are short-hand for derivatives: $h_i = \partial h / \partial \boldsymbol{r}_i$, etc. The first square root expression in Eq. (2) is the metric determinant that accounts for the increased area element if the surface is tilted. The expression following it is the total curvature in Monge gauge. Evidently, the Helfrich Hamiltonian is highly nonlinear in this parametrization! Hence, one frequently expands the integrand for small h, as is done in the second line. The first term, $\frac{1}{2}\kappa(h_{ii})^2 = \frac{1}{2}\kappa(\Delta h)^2$ is quadratic in h and thus gives rise to a harmonic theory, which is referred to as "linearized Monge gauge." The majority of all membrane work relies on this simplified version. However, the higher order terms occasionally matter: they are for instance responsible for the renormalization of the bending rigidity by thermal shape undulations [133 136].

Upon Fourier-transforming $h(\boldsymbol{r}) = \Sigma_{\boldsymbol{q}} \widetilde{h}_{\boldsymbol{q}} \mathrm{e}^{i\boldsymbol{q}\cdot\boldsymbol{r}}$ and restricting the functional to quadratic order we obtain the transformed Hamiltonian $E[\widetilde{h}_{\boldsymbol{q}}] = L^2 \Sigma_{\boldsymbol{q}} \frac{1}{2}\kappa q^4 |\widetilde{h}_{\boldsymbol{q}}|^2$, which shows that the modes $\widetilde{h}_{\boldsymbol{q}}$ are independent harmonic oscillators. The equipartition theorem then implies that $\langle |\widetilde{h}_{\boldsymbol{q}}|^2 \rangle = k_{\mathrm{B}}T / L^2 \kappa q^4$, and thus fitting to the spectrum of thermal undulations gives access to κ. Unfortunately, there are several difficulties with this picture (see, e.g., the recent review [137]). The simple expression can only be expected to hold for sufficiently small wave vectors because at small length scales local bilayer structure will begin to matter. For instance, it is well known that lipid tilt fluctuations contaminate the undulation spectrum [34, 35]. The situation becomes even more complicated in low temperature phases that exhibit hexatic order [138, 139] or permanent tilt [140, 141]. In such cases, the fluctuation spectrum shows no sign of a $\langle |\widetilde{h}_{\boldsymbol{q}}|^2 \rangle \propto 1/q^4$ behavior up to length scales of at least 40 nm [142]. The most obvious way out is to simulate larger systems and thus gain access to smaller wave vectors, but unfortunately these modes decay exceedingly slowly. For overdamped Brownian dynamics with a friction constant $\zeta = L^2 \zeta_0$, one finds $\zeta \dot{\widetilde{h}}_{\boldsymbol{q}} = -\partial E[\widetilde{h}_{\boldsymbol{q}}] / \partial \widetilde{h}_{\boldsymbol{q}} = -L^2 \kappa q^4 \widetilde{h}_{\boldsymbol{q}}$, showing that modes exponentially relax with a time constant $\tau = \zeta_0 / \kappa q^4$ that grows quartically with the wave length. Accounting for hydrodynamics turns this into a cubic dependence, $\tau = 4\eta / \kappa q^3$ [89, 143 145], where η is the solvent viscosity, but the situation is still uncomfortable: when Lindahl and Edholm [15] simulated 1,024 DPPC lipids in a 20 nm square bilayer, their measured value $\kappa = 4 \times 10^{-20}$ J implies $\tau \simeq 3.2$ ns for the slowest (and most informative) mode, not much smaller than the overall 10 ns total simulation time.

Although measuring κ from the undulation spectrum is possible, there is a more basic concern with such an approach: one tries to measure a modulus with a value typically around 20 $k_{\mathrm{B}}T$ by using thermal fluctuations of order $k_{\mathrm{B}}T$ to excite the bending modes, which of course makes it quite challenging to get a signal to begin

with.[2] An obvious alternative is to actively bend membranes and directly measure their curvature elastic response. There are clearly many ways to deform a membrane; here we will describe two possibilities that have been proposed in the past as convenient methods for obtaining the bending modulus.

Harmandaris and Deserno [113] proposed a method that relies on simulating cylindrical membranes. Imagine a membrane of area A that is curved into a cylinder of curvature radius R. Its length L satisfies $2\pi RL = A$, and the curvature energy per area of this membrane is:

$$e = \frac{1}{2}\kappa\frac{1}{R^2} = \frac{1}{2}\kappa\left(\frac{2\pi L}{A}\right)^2 . \tag{4}$$

Because changing the length of the cylinder at constant area will also change the curvature radius, and thus the bending energy, there must be an axial force F associated with this geometry. Its value is given by:

$$F = \left(\frac{\partial eA}{\partial L}\right)_A = A\ \kappa\frac{2\pi L}{A}\ \ \frac{2\pi}{A} = \frac{2\pi\kappa}{R} . \tag{5}$$

Hence, measuring both the axial force and the cylinder radius yields the bending modulus as $\kappa = FR/2\pi$. Notice that within quadratic curvature elasticity, the radius of the cylinder does not matter: Both small and large radii will lead to the same modulus. In other words, FR is predicted to be a constant. Of course, it is conceivable that higher order corrections to the Helfrich Hamiltonian Eq. (1) matter once curvatures become really strong. For the present geometry there is only one term, which enters at quartic order, and one would write a modified energy density $e = \frac{1}{2}\kappa K^2 + \frac{1}{4}\kappa_4 K^4$. This modified functional leads to $FR/2\pi = \kappa + \kappa_4/R^2 \equiv \kappa_{\rm eff}(R)$, which can be interpreted as an effective curvature-dependent bending modulus. Simulations using different models with different levels of resolution have indeed both seen a small dependence of $\kappa_{\rm eff}$ on R [111, 113]. They find softening at high curvature, which would indicate that κ_4 is negative. In contrast, Li et al. [38] recently studied the elastic properties of self-assembled copolymeric bilayers by self-consistent field theory in cylindrical and spherical geometry, and found κ_4 to be positive. The details of nonlinear elastic corrections thus depend on the specifics of the model under study, but the present studies suggest that as long as the radius of curvature is bigger than a few times the membrane thickness, these corrections are negligible. For example, Li et al. [38] found the deviations from linear to be less than 2% both in the cylinder and sphere geometry, as long as the reduced curvature was less than $K_0 d = 0.6$ (where d is the bilayer thickness).

[2] It is easy to see that $\delta h \equiv \langle h(\boldsymbol{r})^2\rangle^{1/2} \quad L\sqrt{k_{\rm B}T/16\pi^3\kappa} \approx L/100$ (assuming $\kappa \simeq 20\, k_{\rm B}T$), which is a few Ångström for typical simulation sizes.

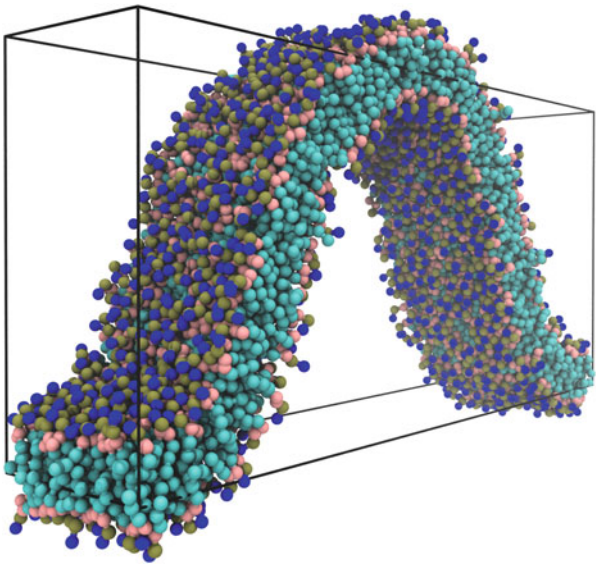

Fig. 1 Illustration of a buckling simulation using the MARTINI model for DMPC (which uses 10 beads per lipid) [116]. This particular membrane consists of 1,120 lipids and is compressed at a strain γ 0.3, which gives it an amplitude of approximately 22% of the box length. To suppress membrane deformations in the second direction, the width of the box is chosen to be much smaller than its length

The cylinder stretching protocol appears to work very well for simple solvent-free membrane models [111, 113, 114], but with more refined models this method suffers from two drawbacks, both related to the equilibration of a chemical potential. First, the cylinder separates the simulation volume into an "inside" and an "outside." If solvent is present, its chemical potential must be the same in these two regions, but for more highly resolved models the solvent permeability through the bilayer is usually too low to ensure automatic relaxation. Second, the chemical potential of lipids also has to be the same in the two bilayer leaflets, and again for more refined models the lipid flip-flop rate tends to be too low for this to happen spontaneously.

To circumvent this difficulty, Noguchi has recently proposed to instead simulate a buckled membrane as an example of an actively imposed deformation [115] (see Fig. 1 for an illustration). This solves both problems simultaneously: neither does the buckle divide the simulation box into two distinct compartments,[3] nor is lipid equilibration across leaflets a big concern because for symmetry reasons both leaflets are identical (at least for a "ground state buckle") and thus ensuring that the same number of lipids is present in both leaflets is a good proxy. The theoretical analysis of the expected forces is a bit more complicated compared to the cylinder setup, but it can be worked out exactly, even for buckles deviating strongly from "nearly flat." Hu et al. have recently provided systematic series expansions for the buckling forces in terms of the buckling strain. If a membrane originally has a

[3] Observe that the part of the membrane above the buckle and the part below the buckle can be connected through the periodic boundary of the simulation box.

length L and is buckled to a shorter length L_x, then the force f_x per length along that membrane as a function of strain $\gamma = (L - L_x)/L$ can be written as [116]:

$$f_x = \kappa \left(\frac{2\pi}{L}\right)^2 \left[1 + \frac{1}{2}\gamma + \frac{9}{32}\gamma^2 + \frac{21}{128}\gamma^3 + \frac{795}{8192}\gamma^4 + \frac{945}{16384}\gamma^5 + \cdots\right]. \quad (6)$$

Notice that the force does not vanish for $\gamma \to 0$, which is the hallmark of a buckling transition. Hu et al. [116] also estimate the fluctuation correction on this result and find it to be very small; they apply this method to four different membrane models, ranging from strongly coarse grained to essentially atomistic, and argue that it is reliable and efficient.

2.3.2 Gaussian Modulus

To measure the Gaussian curvature modulus $\overline{\kappa}$ directly, the Gauss Bonnet theorem [8, 9] forces one to either change the topology or the boundary of a membrane patch. Recently Hu et al. [76, 123] suggested a way to achieve this. Consider a circular membrane patch of area A. Being flat, its energy stems from the open edge at its circumference. The patch could close up into a vesicle in order to eliminate the open edge, but now it carries bending energy. If we imagine that transition proceeding through a sequence of conformations, each one resembling a spherical cap of curvature c, then the excess energy of such a curved patch (compared to the flat state) is given by [7, 146]:

$$\frac{\Delta E(x,\xi)}{4\pi(2\kappa + \overline{\kappa})} = \Delta\widetilde{E}(x,\xi) = x + \xi\left[\sqrt{1-x} - 1\right]. \quad (7)$$

ΔE is scaled by the bending energy of a sphere and we defined:

$$x = (Rc)^2, \quad \xi = \frac{\gamma R}{2\kappa + \overline{\kappa}}, \quad \text{and} \quad R = \sqrt{\frac{A}{4\pi}}\,. \quad (8)$$

For $\xi > 1$ the spherical state ($x = 1$) has a lower energy than the flat state ($x = 0$). If x is viewed as a reaction coordinate, Eq. (7) describes a nucleation process, since for $\xi < 2$ the transition from the flat to the spherical state proceeds through an energy barrier of height $\Delta\widetilde{E}^* = (1 - \xi/2)^2$ at $x^* = 1 - (\xi/2)^2$. Eq. (7) shows that the functional form of the nucleation barrier depends on parameters such as moduli and system sizes only through the combination ξ, and all parameters entering ξ (with the exception of $\overline{\kappa}$) can be determined ahead of time by other means. Hence, measuring $\overline{\kappa}$ amounts to measuring the nucleation barrier (or at least the location of the maximum). Hu et al. [76, 123] do this by a dynamical process: Equilibrated but pre-curved membrane patches with some initial value for x may either flatten out or close up, depending on where on the barrier they start. The

probability for either outcome can be computed if ΔE is known [147] and so $\overline{\kappa}$ ends up being found through a series of patch-closure experiments.

The results of such simulations show that $\overline{\kappa}/\kappa$ is close to -1, both for the Cooke model and for MARTINI DMPC (see Sect. 2.2 for a further discussion of these models).[4] This is compatible with experiments [117 122] but disagrees with the only other method that has been suggested for getting the Gaussian modulus. As first pointed out by Helfrich [148], quite general considerations suggest that the second moment of a membrane's lateral stress profile is also equal to the Gaussian modulus [148 150]:

$$\overline{\kappa} = \int \mathrm{d}z \; z^2 \Sigma(z), \tag{9}$$

where $\Sigma(z) = \Pi_{zz} - \frac{1}{2}\left[\Pi_{xx}(z) + \Pi_{yy}(z)\right]$ is the position-resolved lateral stress through a membrane, whose integral is simply the surface tension [151]. However, when applied to the Cooke model, Hu et al. find $\overline{\kappa}/\kappa \approx -1.7$ [76], which quite a bit more on the negative side, whereas applying it to MARTINI DMPC (at 300 K) yields $\overline{\kappa}/\kappa \approx -0.05$, much closer to zero; MARTINI DPPC and DOPC (dioleoylphosphatidylcholine) even lead to positive Gaussian moduli. At present it is unclear where this discrepancy originates from, but given that the values obtained from the patch-closure protocol are physically more plausible it seems likely that there is a problem with the stress approach. The latter suspicion is also supported by the fact that a more refined theory of bilayer elasticity [152] predicts corrections to the right-hand side of Eq. (2) that depend on moments of order parameter distributions.

2.4 The Tension of Lipid Membranes

The Helfrich Hamiltonian, Eq. (1), does not include a surface tension contribution. Free membrane patches can relax and adjust their area such that they are stress-free. In many situations, however, membranes do experience mechanical stress. For example, an osmotic pressure difference between the inside and the outside of a lipid vesicle generates stress in the vesicle membrane. Stress also occurs in supported bilayer systems, or in model membranes patched to a frame. In contrast to other quantities discussed earlier (bending stiffness etc.), and also in contrast to the surface tension of demixed fluid phases, membrane stress is not a material parameter. Rather, it is akin to a (mechanical or thermodynamic) control parameter, which can be imposed through boundary conditions.

The discussion of membrane tension is complicated by the fact that there exist several different quantities that have been called "tension" or "tension-like." For the sake of simplicity, we will restrict ourselves to quasiplanar (fluctuating)

[4] The requirement that the Hamiltonian (1) is bounded below demands that $2\kappa \leq \overline{\kappa} \leq 0$.

membranes in the following. A thoughtful analysis of the vesicle case has recently been carried out by Diamant [153].

The first tension-like quantity in planar membranes is the lateral mechanical stress in the membrane, as discussed above. If the stress is imposed by a boundary condition, such as, for instance, a constraint on the lateral (projected) area of the membrane, it is an internal property of the membrane system that depends, among other parameters, on the area compressibility [36] and the curvature elasticity [154 161]. Alternatively, mechanical stress can be imposed externally. In that case, the projected area fluctuates, and the appropriate thermodynamic potential can be introduced into the Helfrich Hamiltonian, Eq. (1), in a straightforward manner:

$$G = E - \Gamma_{\text{frame}} A_{\text{p}} = \int_{\mathcal{S}} \mathrm{d}A \ \left\{ \frac{1}{2}\kappa (K - K_0)^2 + \overline{\kappa} K_{\text{G}} - \Gamma_{\text{frame}} \frac{\mathrm{d}A_{\text{p}}}{\mathrm{d}A} \right\}. \tag{10}$$

Here Γ_{frame} is the stress or "frame tension," A_{p} is the projected area in the plane of applied stress, and we have omitted the membrane edge term. Let us consider a membrane with fixed total area A. In Monge representation, one has $\mathrm{d}A_{\text{p}}/\mathrm{d}A = 1/\sqrt{1 + (\nabla \mathrm{h})^2} \approx 1 - (\nabla h)^2/2 + \mathcal{O}\left(h^4\right)$, thus the last term in Eq. (10) takes the form [37, 162]:

$$\text{const} + \frac{1}{2}\Gamma_{\text{frame}} \int_{A_{\text{p}}} \mathrm{d}^2 r \ \ (\nabla h)^2 + \mathcal{O}\left(h^4\right) \tag{11}$$

(with const $= -\ \Gamma_{\text{frame}} A$). This is formally similar to a surface tension term in an effective interface Hamiltonian for liquid liquid interfaces. The main difference is that the base A_{p} of the integral fluctuates. However, replacing this by a fixed base $\langle \mathrm{A_p} \rangle$ only introduces errors of order $\mathcal{O}\left(h^4\right)$ [162].

From Eq. (11), it is clear that mechanical stress influences the fluctuation spectrum of membranes and, in particular, one expects a q^2 contribution to the undulation spectrum, $\langle |\widetilde{h}_q|^2 \rangle \ ^1 \sim \Gamma_{\text{fluc}} q^2 + \kappa q^4 + \cdots$. This introduces the second tension-like parameter in planar fluctuating membranes, the "fluctuation tension" Γ_{fluc}. According to Eq. (11), Γ_{fluc} is identical to Γ_{frame} up to order $\mathcal{O}\left(h^2\right)$.

Finally, the third tension-like parameter in membranes was introduced by Deuling and Helfrich as early as 1976 [163], and it couples to the total area of the membrane:

$$E = \int_{\mathcal{S}} \mathrm{d}A \ \left\{ \frac{1}{2}\kappa (K - K_0)^2 + \overline{\kappa} K_{\text{G}} + \Gamma_0 \right\}. \tag{12}$$

In membranes with fixed lipid area, but variable number of lipids, the "bare tension" Γ_0 is simply proportional the lipid chemical potential. For membranes with fixed number of lipids and variable lipid area, the physical meaning of Γ_0 is less clear, but it can still be defined as a field that is conjugate to A in a Lagrange multiplier sense. This term also gives rise to a q^2 term in the undulation spectrum, with the fluctuation tension $\Gamma_{\text{fluc}} = \Gamma_0 + \mathcal{O}\left(h^2\right)$ [36].

At leading (quadratic) order in h, the three tension-like quantities, Γ_{frame}, Γ_{fluc}, and Γ_0, thus have identical values. Nevertheless, they might differ from each other due to nonlinear corrections [90, 164 167]. For instance, the bare tension Γ_0 is expected to deviate from the frame tension Γ_{frame} due to the effect of fluctuations. The exact value of the correction depends on the ensemble and differs for systems with a fluctuating number of lipids (variable number of undulating modes) or a fixed number of lipids (fixed number of modes). The former case was analyzed by Cai et al. [165] and the latter case by Farago and Pincus [168] and subsequently by a number of other authors [169 171]. Interestingly, the correction has an additive component in both cases. Hence a stress-free membrane has a finite bare tension.

Whereas the bare tension Γ_0 is mostly of academic interest, the fluctuation tension Γ_{fluc} describes actual membrane conformations. The relation between Γ_{fluc} and Γ_{frame} has been discussed somewhat controversially in the past [153, 156, 162, 165, 169 174]. Cai et al. [165] and Farago and Pincus [156] have presented a very general argument for why Γ_{frame} and Γ_{fluc} should be equal. Cai et al. [165] examined the fluctuations of planar membranes with variable number of lipids and fixed lipid area and proved $\Gamma_{\text{fluc}} = \Gamma_{\text{frame}}$ in the thermodynamic limit, if the membrane is "gauge invariant," i.e., invariant with respect to a rotation of the "projected plane." Farago and Pincus [156, 174] developed a similar theory for membranes with fixed number of lipids at fixed projected area. Unfortunately, these arguments albeit appealing are not entirely conclusive because the underlying assumptions can be questioned: The thermodynamic limit does not exist for stress-free planar membranes because they bend around on length scales larger than the persistence length [90]. In the presence of stress, the limit does not exist either, strictly speaking, because the true equilibrium state is one where the membrane has ruptured. Furthermore, high stresses break gauge invariance. Contradicting Cai et al. and Farago and Pincus [156, 165], a number of authors have claimed $\Gamma_{\text{fluc}} = \Gamma_0$ [169 171], based on analytical arguments that, however, also rely on the existence of the thermodynamic limit and on other uncontrolled approximations [162, 172, 173].

Thus, the relation between Γ_{frame} and Γ_{fluc} remains an open question, and simulations can point at the most likely answer. For example, if $\Gamma_{\text{fluc}} = \Gamma_{\text{frame}}$, the fluctuation tension should vanish for stress-free membranes, i.e., the undulation spectrum should then be dominated by a q^4 behavior. With a few exceptions [169, 170], this has indeed been observed in coarse-grained or atomistic simulations of stress-free lipid bilayers [12, 15, 28, 30, 109, 175] or bilayer stacks [176]. This would seem to rule out the alternative hypothesis $\Gamma_{\text{fluc}} = \Gamma_0$. However, it should be noted that the undulation spectra have relatively large error bars and a complex behavior at higher q, as discussed in Sect. 2.3.1. Therefore, the results also depend to some extent on the fit.

To overcome these limitations, accurate simulations of elastic infinitely thin sheets with no molecular detail are useful. Recently, a number of such simulations have been carried out in two spatial dimensions (i.e., one dimensional membranes) [162, 171, 174]. The results are found to depend on the ensemble. Fournier and Barbetta studied a membrane made of hypothetical "lipids" with freely fluctuating

areas, only controlled by a Lagrange parameter Γ_0. They found that the fluctuation tension Γ_{fluc} displays a complex behavior and neither agrees with Γ_0 nor with Γ_{frame}. Schmid [162] has considered an arguably more realistic situation where "lipids" have fixed area and either a fixed frame tension is applied or the "projected area" is kept fixed. These simulations reproduce the difference between Γ_0 and Γ_{frame} and indicate with high accuracy that the fluctuation tension is given by $\Gamma_{\text{fluc}} = \Gamma_{\text{frame}}$. Farago [174] confirmed these findings in simulations at fixed projected area. Furthermore, he carried out reference simulations of a hypothetical membrane model that lacks gauge invariance and found that, in this case, the fluctuation tension deviates from the frame tension. These studies support the validity of the picture originally put forward by Cai et al. [165]: For rotationally invariant membranes with fixed area per lipid, the fluctuation tension is given by the frame tension.

2.5 *Membrane Heterogeneity and Lipid Rafts*

In the late 1990s, several scientists put forward the suggestion that biomembranes might not be laterally homogeneous but instead contain nanoscopic domains soon called "lipid rafts" which differ in their lipid composition and are important for numerous membrane-associated biological processes [177 181]. This idea quickly replaced the prevailing fluid mosaic model [182], according to which the lipid bilayer merely constitutes a two-dimensional passive solvent that carries membrane proteins. It created huge excitement due to many obvious biological implications and possibilities; at the same time it was controversial, for instance because it took time to converge on a universally accepted definition of what a raft is [82, 183 185].

According to the lipid raft concept, biomembranes are filled with locally phase-separated, cholesterol-rich, nanoscale "raft" domains, which contribute to membrane heterogeneity and play an important role in organizing the membrane proteins. Two aspects of this hypothesis are well-established: First, biological membranes are laterally heterogeneous, and heterogeneity is important for the function of membrane proteins, e.g., in signaling [186]. Second, multicomponent lipid bilayers phase separate in certain parameter regions into a "liquid disordered" (ld) and a "liquid ordered" (lo) phase [187, 188]. The hypothetical "raft state" is not phase-separated, but rather a globally homogeneous state filled with nanodomains of sizes between 10 and 100 nm. The raft concept is supported by experimental findings, e.g., on the mobility of certain membrane proteins [189]. It has been questioned mainly due to a lack of direct evidence. Rafts are too small to be visualized in vivo by microscopy. Moreover, it was not clear from a theoretical point of view why nanoscale rafts should be stable with respect to macrophase separation. To explain this, it was proposed that rafts might be nonequilibrium structures [190] and that rafts might be stabilized by the cytoplasm [191] or by special line-active lipids [192 194]. Alternatively, it was argued that rafts

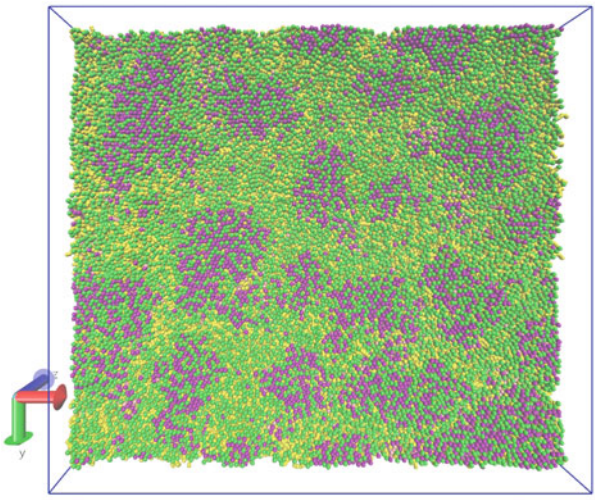

Fig. 2 Rafts in a two component lipid bilayer (20,000 lipids, Lenz model). Purple *(darker)* beads correspond to cholesterol and green *(lighter)* beads to phospholipids (see [81])

might simply be a signature of critical fluctuations in the vicinity of critical points [195, 196].

Whether a thermodynamically stable nanostructured raft state could exist in simple multicomponent membranes that do not contain special line-active additives has remained unclear until recently. This theoretical question mark could be removed by recent simulations of the two-component Lenz model by Meinhardt et al. [81]. Figure 2 shows a top view of a configuration that contains microscopic cholesterol-rich domains. The simulations were carried out in a grand canonical ensemble where lipids and cholesterol can swap identities, which excludes the possibility that the finite domains simply reflect incomplete phase separation. The lateral structure factor of the membranes exhibits a peak at around $q \sim 0.08\ \mathrm{nm}^{-1}$. Its existence shows that the clusters are not critical. Hence, raft-like structures can be thermodynamically stable in multicomponent membranes. The characteristic length scale of roughly 12 nm is compatible with the size commonly attributed to lipid rafts in biomembranes [82].

Two comments are in place here. First, it should be noted that typical "raft mixtures" used for studying rafts in model membranes contain at least three components. This is because three components seem necessary to bring about global lateral phase separation [188]. Meinhardt et al. report raft-like structures in simulations of a coarse-grained model for binary mixtures but, as in experiments, their systems do not show global phase separation between fluid states. Likewise, there is also some experimental evidence that nanoscopic domains may already be present in binary mixtures in particular mixtures of saturated lipids (lipids with high main transition temperature) and cholesterol. Studies based on local techniques such as ESR, NMR, or diffusitivy measurements have indicated the existence of immiscible liquid phases [188, 197, 198], whereas in fluorescence microscopy, one only observes one homogeneous phase [188]. This suggests that

these two-component membranes phase-separate on the nanoscale, while remaining homogeneous on the global scale, and that they thus feature many of the intriguing properties attributed to rafts.

Second, the characteristic length scale of the rafts is similar to the wavelength of the ripple state in one-component bilayers in the transition region between the fluid and the tilted gel $L_{\beta'}$ state [199, 200]. Experimentally [201, 202] and in computer simulations [80, 203 207], modulated phases are observed in lipid bilayers that exhibit a tilted gel state, and they are not observed in lipid bilayers with an untilted gel state L_β [201 203, 208]. For example, in the Lenz model, rippled states occur in the standard setup with a mismatch between head and tail size [80], but they disappear if the head size is reduced such that the tilt in the gel phase vanishes [208].

Meinhardt et al. [81] have proposed a joint theoretical explanation for these findings, which is based on the coupled monolayer model (see Sect. 2.1.3). They assumed that monolayers exhibit local phase separation into two phases with different order parameter (composition or other), and that the spontaneous curvature of the monolayer depends on the local order parameter. In the strong segregation limit where different phases are separated by narrow interfaces, they showed that the line tension is reduced in the presence of a mismatch ΔK_0 between the spontaneous curvatures of the two phases. This is because monolayers with a spontaneous curvature, which are forced into being planar by the apposing monolayer, experience elastic stress, and some of that stress can be released at the domain boundaries. The resulting negative contribution to the line tension scales with $\kappa\,(\Delta K_0)^2$ and should be present wherever ΔK_0 is nonzero. A more detailed calculation shows that the elastic energy is minimized for circular or stripe domains of a specific size, which is of the order of a few nanometers. This elastic mechanism could thus stabilize rafts of finite size for sufficiently large spontaneous curvature mismatch.

Meinhardt et al. also considered the weak segregation limit, where the phase separation is incomplete, the interfaces are broad, and the free energy can be expanded in powers of the order parameter Φ. They showed that the expansion has a Landau Brazovskii form [209]:

$$F = \int \mathrm{d}^2 r \left\{ \frac{g}{2} \left(\Delta + q_0^2\right)^2 \Phi^2 + \frac{r}{2}\Phi^2 - \frac{\gamma}{3!}\Phi^3 + \frac{\lambda}{4!}\Phi^4 \right\}, \tag{13}$$

with a characteristic wave vector of the order $q_0 < 1/\xi$, where ξ is the in-plane correlation length $\xi = (\kappa t_0^2/K_A)^{1/4}$ (t_0 is the monolayer thickness and K_A the area compressibility). The Landau Brazovskii model describes phase transitions driven by a short-wavelength instability between a disordered and one or several ordered phases. In mean-field approximation, it predicts a transition from a disordered phase to one of several ordered modulated phases (lamellar or hexagonal). Fluctuations are known to shift the order disorder transition and to stabilize a locally structured disordered phase via the so-called Brazovskii mechanism [209]. The

correlation length ξ sets the order of magnitude and a lower limit for the characteristic wave length of the structures. Inserting typical numbers for the elastic parameters of DPPC bilayers in the fluid phase, one obtains $\xi \sim 1$ nm.

The simple theory put forward by Meinhardt et al. accounts in a unified manner for both ripple phases and raft states in membranes. The prerequisites for the formation of such modulated phases is local phase separation (e.g., in the ripple case, between a liquid and a gel phase, or in the raft case, between a liquid disordered and a liquid ordered phase) and curvature stress in at least one of the two phases (typically the ordered one), resulting, e.g., from a size mismatch between head group and tails. In order to reproduce rippled states or rafts, coarse-grained simulation models must meet these criteria. This is often not the case. For example, the standard version of the popular MARTINI model does not have a ripple phase, because the low-temperature gel phase of saturated phospholipids is untilted.

3 Membrane–Protein Interactions

Biomembranes achieve their biological functions through a multitude of membrane-associated proteins. Whereas the membranes were long thought to mainly serve as a more or less inert background matrix for these proteins, the interactions between membranes and proteins have received more and more attention in recent years [210]. Membranes can affect protein function in several ways. The local lipid environment can immediately influence the function of proteins, e.g., by influencing the tilt and relative position of transmembrane domains [211] or by exerting local pressure on proteins [212]. Furthermore, membranes contribute to the effective interactions between proteins [213 215], and they can be used to tune protein clustering. In mixed membranes, the "raft hypothesis" mentioned in Sect. 2.5 asserts that nanoscale lipid domains in membranes help to organize and control protein assembly [82, 178].

Membrane protein interactions are controlled by various factors: Local lipid packing, local lipid concentration, membrane distortion, and monolayer and bilayer elasticity. Proteins are surrounded by a shell of lipid molecules (the lipid annulus), which mostly interact nonspecifically with the protein molecules [216]. Protein membrane interactions are thus to a large extent determined by the interactions of the annuli with the bulk, and often do not depend strongly on the details of the protein sequences. If membrane proteins locally deform the lipid bilayer to which they are bound, this can induce forces between them that are potentially long-ranged and quite universal in their characteristics. The reason is that the bilayer acts as a field that can transmit local perturbations, and thus forces, to distant regions. This is perfectly analogous to the way in which for instance an electrostatic field mediates interactions between electric charges or curved space time mediates interactions between masses, except that a membrane seems more tangible than the other examples. However, once we look beyond

fundamental forces towards higher level emergent phenomena, very tangible fields exist everywhere. For instance, a rope can transduce a tensile force along its length, and we can describe this using continuum elasticity as the underlying "field equation."

Just like ropes, fluid lipid membranes are continuous media at a sufficiently coarse level of description. But, their rich physical structure equips them with several properties that can take on the role of a field, for instance:

1. The membrane thickness can be considered as a spatially varying field that couples to the protein content (see Sect. 2.1.3)
2. The lipids can have a spatially varying orientation or tilt order
3. In mixed membranes, the local lipid concentrations can be viewed as a field
4. The Hamiltonian Eq. (1) associates a characteristic energy to a given shape of a membrane, thus rendering its entire geometry a field

These fields differ quite substantially in their theoretical description: concentrations are *scalar* variables, orientations are *vectors*, and differential geometry is at heart a *tensor* theory; but, all of them are known to mediate interactions. For instance, the fact that proteins might prefer one lipid composition over another and thus aggregate [217 220] is central to an important mechanism attributed to lipid rafts. Tilt-mediated protein interactions have also been studied in multiple contexts [32, 33, 159, 221 223]. It is even possible to describe all these phenomena within a common language [224], using the framework of covariant surface stresses [154, 155, 157 161]. However, in the present review we will restrict the discussion to only two examples, both related to membrane elasticity: in Sect. 3.1 we will discuss interactions due to hydrophobic mismatch, and in Sect. 3.2 we will look at interactions mediated by the large-scale curvature deformation of the membrane.

3.1 Hydrophobic Mismatch

Proteins distort or disrupt membranes, which in turn act back on proteins. Structural perturbations contribute to protein function and are among the most important sources of membrane-induced interactions between proteins. Unfortunately, perturbations or transformations of lipid bilayers due to proteins are very difficult to probe experimentally [225]. Complementary theoretical and computer simulation studies can help to elucidate the role of the lipid bilayer in processes such as protein aggregation and function.

One major source of membrane protein interactions that has been discussed in the literature for many decades is hydrophobic mismatch [20 22, 24, 26, 28, 29, 226 233]. If the width of the hydrophobic transmembrane domain of a protein is larger than the thickness of the lipid bilayer, the system can respond in two ways: either the protein tilts [234 236] or the membrane deforms [18, 23, 24]. Both responses have biologically relevant consequences. On the one hand, the

orientation of proteins is believed to have a significant influence on their functionality, e.g., in pore formation [237]. Coarse-grained simulations by Benjamini and Smit have suggested that the cross-angle distributions of packed helix complexes are mostly determined by the tilt angle of individual helices [211]. Membrane deformation, on the other hand, induces effective protein protein interactions and provides one way to control protein aggregation [229, 230, 238]. In experimental tilt measurements, hydrophobically mismatched proteins were sometimes found to tilt; in other cases, the reported tilt angles were surprisingly small compared to theoretical expectations [239 241]. This was partly attributed to problems with the analysis of experimental NMR (nuclear magnetic resonance) data [233] and partly to the presence of anchoring residues flanking the hydrophobic transmembrane domains, which might prevent tilting through a variety of mechanisms [236, 240, 242, 243].

However, coarse-grained simulations show that the propensity to tilt is also influenced by more generic factors. Venturoli et al. have reported that cylindrical inclusions with larger radius tilt less than inclusions with small radius [234]. Neder et al. have identified hydrophobicity as another crucial factor determining tilt [244]. In systematic studies of a variety of simple inclusions with cylindrical shape and similar radii, embedded in a model bilayer of the Lenz type, they found that the behavior of different proteins mainly depended on their free energy of insertion, i.e., their binding free energy. Weakly hydrophobic inclusions with negative binding free energies (which stayed inside the membrane due to kinetic free energy barriers) react to hydrophobic mismatch by tilting. Strongly hydrophobic inclusions with binding energies in excess of 100 k_BT deform the membrane. For the probably most common weakly bound inclusions with binding energies of around 10 k_BT, the situation is more complicated: upon increasing hydrophobic mismatch, inclusions first distort the bilayer and then switch to a tilted state once a critical mismatch parameter is reached. Tilting thus competes with the formation of dynamic complexes consisting of proteins and a shell of surrounding, stretched lipids, and the transition between these two states was found to be discontinuous.

In the case where the membrane is deformed, the deformation profiles can be compared to a variety of theories [16, 17, 27, 33, 245 247]. Both in coarse-grained [30, 234] and atomistic [248] simulations, it was reported that membrane thickness profiles as a function of the distance to the protein are not strictly monotonic, but exhibit a weakly oscillatory behavior. This feature is not compatible with membrane models that predict an exponential decay [16, 17, 27], but it is nicely captured by the coupled elastic monolayer models discussed earlier [22, 28, 30]. Coarse-grained simulations of the Lenz model showed that the coupled monolayer models describe the profile data at a quantitative level, with almost no fit parameters except the boundary conditions [30, 244].

In membranes containing several inclusions, the membrane thickness deformations induce effective interactions between inclusions. These have also been studied within the Lenz model [30, 249] and other coarse-grained models [250, 251]. The comparison with the elastic theory is less convincing, due to the fact that

many other factors such as local lipid packing contribute to the effective potential of mean force, which cannot easily be separated from the pure hydrophobic mismatch contribution [30]. Except for inclusions with very large radii [251], the hydrophobic mismatch contribution to the effective interactions was generally found to be attractive.

3.2 Curvature-Mediated Interactions Between Proteins

3.2.1 The Mystery of the Sign

A very striking experimental demonstration of membrane curvature-mediated interactions was given by Koltover et al. in 1999 [252]. These authors mixed micron-sized colloidal particles with giant unilamellar vesicles to which they could adhere. In the absence of vesicles, the colloidal particles showed no tendency to aggregate in solution, whereas they quickly did once they adsorbed onto the vesicles. Since it was also evident from many micrographs that the colloids induced local bending of the vesicle's membrane, the experiment strongly pointed towards membrane curvature-mediated attractions between the adhering colloids. This, however, was very surprising. Although interactions were indeed expected, the force should have been repulsive, as predicted 6 years earlier by Goulian et al. [253]. Interestingly, the prefactor of this interaction had to be corrected twice [254, 255], but this did not change the outcome: the colloids should have repelled. It was soon understood that objects that cause anisotropic deformations could in fact orient and then attract [256 258], but the colloids of Koltover et al. were isotropic (as far as one could tell experimentally).

We will try to provide a glimpse into this mystery. A big part of it has to do with careless use of the statement "theory has predicted." Theory always deals with model systems and makes simplifying assumptions, and this particular problem is fraught with seemingly inconsequential details that could and sometimes do matter.

3.2.2 The Nonlinear Ground State: Take I

The relevant field Hamiltonian pertaining to the curvature-mediated interaction problem is Eq. (1), minus several terms that will not matter. For a start, the last term involving the edge tension γ does not arise in the absence of any membrane edge. The spontaneous bilayer curvature K_0 usually vanishes for symmetry reasons. If lipids can flip between the two leaflets, their chemical potential must be the same in both, and if no other symmetry-breaking field is present, this means that $K_0 = 0$. Unfortunately, membrane curvature itself breaks the bilayer symmetry, and any existing lipid composition degree of freedom must couple to the geometry [75, 259 263]. So let us for now assume that this is not the case and take a note of

this first nontrivial assumption. Moreover, in actual biomembranes, none of this need be true because active and passive processes can maintain an asymmetric lipid composition across the two leaflets [264, 265]. Finally, the term involving the Gaussian curvature can be dropped here because we will encounter neither edges nor topology changes, and so the Gauss Bonnet theorem will work in our favor.

What remains is the simpler Hamiltonian Eq. (2), but this looks quite formidable in Monge parametrization. To make any progress with something as forbidding as this appears quite unlikely. And yet, not all hope is lost. For a spherical particle attached to an asymptotically flat membrane, the nonlinear shape equation has an exact solution, namely, a catenoid. This is an axisymmetric minimal surface with $K \equiv 0$ and hence obviously minimizes the left-hand side of Eq. (2). If one adds additional lateral membrane tension, the exact shape of the membrane around a single adhering spherical particle can no longer be calculated analytically, but numerical solutions are relatively easy to come by using an angle arc length parametrization [266]. Unfortunately, we need to know the solution for two particles, and in the absence of axisymmetry this is difficult, even numerically. It has been done [267], but before we discuss this approach, let us first see what results we can analytically wrest from these equations.

Even for the full nonlinear problem, the tight link between geometry and surface stress permits one to express mediated interactions as line integrals over the equilibrium membrane geometry. For instance, picture two spherical particles bound to a membrane, held at some mutual distance. If the particles are identical, then this will give rise to a mirror-symmetric membrane shape, and it can be shown that the force between these particles can be written as [158, 159]:

$$F = \frac{1}{2}\kappa \int \mathrm{d}s \ \left\{K_{\perp}^2 - K_{||}^2\right\}, \tag{14}$$

where for simplicity we restrict to the tensionless case. The integral runs across the symmetry curve (the intersection of the membrane with the mirror plane), $K_{||}$ is the local curvature of that curve and $K_{\perp}$ the local curvature perpendicular to that curve. The sign convention is such that a negative sign implies attraction. To obtain an interaction strength out of Eq. (14) we need these curvatures, for which we need to solve the shape equations after all. Unfortunately, not even the sign of the interaction is evident from Eq. (14), since the difference of two squares enters the integrals. Had we been curious instead about the interaction (per unit length) between two parallel rods on the membrane, we would have been in a better position: Now $K_{||}$ would be zero and the interaction would be clearly repulsive (even though we still do not quite know how strong it is). It seems that in order to make headway, we must solve the shape equation. The only hope of doing this in reasonable generality using analytical tools is to linearize it.

3.2.3 Linearization and Superposition Approximation

Linearizing the nonlinear geometric functional means restricting to the first term in the integrand of Eq. (3). If we add a surface tension Γ, this means looking at the energy density $\frac{1}{2}\Gamma(\nabla h)^2 + \frac{1}{2}\kappa(\Delta h)^2$, where ∇ and Δ are the two-dimensional (flat!) surface gradient and Laplacian, respectively. A functional variation yields:

$$[-\Gamma\Delta + \kappa\Delta\Delta]\ h(\boldsymbol{r}) = 0\ . \tag{15}$$

This shape equation is of fourth order, but it is linear. Unfortunately, in the present context we must solve it for a two-particle problem with finite-sized particles, and therein lies the rub: the operator in square brackets is not separable in any simple coordinate system, so we have to deal with the fact that this equation is indeed a partial differential equation.

A popular trick to avoid this problem rests on the following reasoning: If the equation is linear, one might first want to look for a solution of the one-particle problem and then simply create the two-particle solution by superposition. We can then apply Eq. (14) to calculate the force, which in the present example would yield the interaction potential [224]:

$$U(r) = 2\pi\kappa\ \widetilde{\alpha}^2\ \mathrm{K}_0(r/\lambda) \quad \text{with} \quad \lambda = \sqrt{\frac{\kappa}{\Gamma}} \qquad \text{and}\ \widetilde{\alpha} = \frac{\alpha}{\mathrm{K}_1(r_0/\lambda)}\ . \tag{16}$$

Here, r is the distance between the particles, r_0 is the radius of the circular contact line at which the membrane detaches from the colloid, α is the angle with respect to the horizontal at which it does so, and the K_ν are modified Bessel functions of the second kind. This solution is analytical, simple, and wrong. Or more accurately, it only holds when $r \gg \lambda \gg r_0$, a restriction that excludes the interesting tensionless limit in which $\lambda \to \infty$. The mathematical reason is that superposition in the way celebrated here is not allowed: yes, superpositions of solutions to linear equations are still solutions, but superpositions of solutions, each of which only satisfies some part of all pertinent boundary conditions, generally do not satisfy any boundary condition and are thus not the solutions we are looking for. The physical reason why the superposition ansatz in this case fails is because the presence of one colloid on the membrane, which creates a local dimple, will abet a nearby colloid to tilt, thereby changing the way in which that second colloid interacts with the membrane and, in turn, the first one.

3.2.4 Linearization and a Full Two-Center Solution

One way to circumvent the superposition approximation is to solve the full two-center problem. This is of course much more tedious, and in fact can only be handled as a series expansion, in which one satisfies the boundary conditions at both

particles up to some order in the multipoles, and an expansion in the smallness parameter r_0/r. This calculation has been done by Weikl et al. [268], leading to:

$$U(r) = 2\pi\kappa\left(\frac{\alpha r_0}{\lambda}\right)^2\left\{K_0(r/\lambda) + \left(\frac{r_0}{\lambda}\right)^2 K_2^2(r/\lambda) + \cdots\right\}. \tag{17}$$

Notice that in the case $r \gg \lambda \gg r_0$ this indeed reduces to Eq. (16), whereas in the more interesting limit in which the tension vanishes it reduces to:

$$U(r) = 8\pi\kappa\alpha^2\left(\frac{r_0}{r}\right)^4, \tag{18}$$

which is indeed the solution of Goulian et al. [253], amended by the prefactor corrections [254, 255]. In fact, these authors have actually written down the solution for the case of two nonidentical particles 1 and 2 with detachment angles α_1 and α_2. If we also make their radii r_i different, we find [269]:

$$U(r) = 4\pi\kappa\left(\alpha_1^2 + \alpha_2^2\right)\frac{r_1^2 r_2^2}{r^4}. \tag{19}$$

Notice that, unlike what one might have guessed from Eq. (18), the potential (and thus the force) is not proportional to the product of the two detachment angles. The actual form of the prefactor, $\alpha_1^2 + \alpha_2^2$, is highly suggestive of an entirely different underlying physics, as we will now see.

3.2.5 Linearization Using Effective Field Theory

Equations (17), (18), and (19) are expansions of the exact solution for large distance. Working out higher order terms appears reasonably forbidding, given that one has to push a difficult multicenter problem to a high order. However, there is a way to disentangle the multicenter problem from the interaction problem.

We have seen that the physical reason why the superposition approximation fails is the induced tilting of neighboring colloids. More generally, any finite particle in contact with the membrane will induce extra membrane deformations if the membrane in its vicinity is perturbed. This is simply a polarization effect: Any "incoming" field interacts with the boundary conditions imposed by the particle and these then create new "outgoing" fields. Superposition of fields would work for point particles, but these do not capture the polarization effects, unless we equip them with the requisite polarizabilities. But this of course we can do. We can write a new Hamiltonian of interacting point particles, where each of them has the same polarizabilities as the actual finite size particles of the situation we actually wish to describe. This works by adding terms to the Hamiltonian that are localized at the position of the particle and that couple to the field in the same way that a local polarizability would. For instance, if a particle at the position r_α has a dipole

polarizability $C_\alpha^{(1)}$, we must add the term $\frac{1}{2}C_\alpha^{(1)}[h_i(\boldsymbol{r}_\alpha)]^2$ to the Hamiltonian, where the index i is again a derivative. The energy increases quadratically with the gradient of the local field exactly as for a dipole polarizability. The only remaining question is: where do we get the polarizabilities from? The answer is, just like in classical electrostatics, by calculating the response of one particle in a suitably chosen external field and comparing the full theory with the effective point particle theory.

This idea is an example of what is referred to as effective field theory [270], and it has been used for a host of vastly diverse problems, ranging from black holes in general relativity [271, 272] to finite-size radiation corrections in electrodynamics [273]. The first application in the context of fluid soft surfaces was given by Yolcu et al. [274, 275]. For two axisymmetric particles on a membrane, Yolcu and Deserno showed that Eq. (19) extends as follows [269]:

$$U(r) = 4\pi\kappa\left(\alpha_1^2 + \alpha_2^2\right)\frac{r_1^2 r_2^2}{r^4} + 8\pi\kappa\left(\frac{\alpha_1}{r_1} - \frac{\alpha_2}{r_2}\right)^2 \frac{r_1^4 r_2^4}{r^6} + \cdots \tag{20}$$

Notice that the next order correction is also repulsive and in fact vanishes for identical particles (in contrast to some earlier calculations [276] that missed terms that contribute at the same order).

3.2.6 Fluctuation-Mediated Interactions

It has long been known that even two flat circular particles on a membrane feel an interaction because their boundaries affect the fluctuation spectrum of the membrane and thus its free energy. These forces are proportional to the thermal energy $k_\mathrm{B}T$ and not to the surface rigidity κ and are examples of Casimir interactions in soft matter systems [277]. For circular discs on a tensionless membrane the forces are attractive and, to lowest order, decay like the fourth power of distance [253, 276, 278, 279].

The true beauty of the effective field theory approach described in the previous section is that it also greatly simplifies force calculations on thermally fluctuating surfaces [269, 274, 275]. For two flat rigid particles of radii r_1 and r_2, Yolcu and Deserno find [269]:

$$-\frac{U(r)}{k_\mathrm{B}T} = 6\,\frac{r_1^2 r_2^2}{r^4} + 10\,\frac{r_1^2 r_2^4 + r_1^4 r_2^2}{r^6} + 3\,\frac{r_1^2 r_2^2\left(5r_1^4 + 18 r_1^2 r_2^2 + 5r_2^4\right)}{r^8} + \cdots . \tag{21}$$

The leading order is well known,[5] all higher orders are new. In fact, if one restricts to identical particles, many more orders can be readily written down:

[5] Unfortunately, in the first paper that discusses this force, Goulian et al. [253] claim that the prefactor is 12, a mistake that is not fixed during the prefactor fixing in [254].

$$-\frac{U(r)}{k_B T} = \frac{6}{x^4} + \frac{20}{x^6} + \frac{84}{x^8} + \frac{344}{x^{10}} + \frac{1388}{x^{12}} + \frac{5472}{x^{14}} + \frac{21370}{x^{16}} + \frac{249968}{x^{18}} \cdots, \qquad (22)$$

where $x = r/r_0$.

So here we have the first example of an attraction. Could these forces explain the aggregation observed by Koltover et al. [252]? This is difficult to say. First, in the case of almost flat membranes, which all these calculations implicitly assume by using linearized Monge gauge, the ground state repulsion, Eq. (19), overwhelms the fluctuation contribution, Eq. (21), once $\alpha > \alpha_c = \sqrt{3 k_B T / 4\pi\kappa}$. For a typical choice of $\kappa = 20\, k_B T$ this gives the rather small angle $\alpha_c \approx 6^\circ$. Most likely the colloids in the experiments by Koltver et al. imposed much bigger deformations, but it is hard to say what happens to both forces at larger angles. In the next section, we discuss the numerical solution of the ground state problem, but at present no calculations exist that push the Casimir force beyond the linear regime, except in the case of two parallel cylinders, for which Gosselin et al. find, rather remarkably, that the Casimir force is repulsive [280].

3.2.7 The Nonlinear Ground State: Take II

The various linear calculations show that two axisymmetric colloids on a membrane should repel. But, as the detachment angles α_i increase, it becomes harder to justify the linearization. The expansion in Eq. (3) ultimately rests on the smallness of $|\nabla h|$, an expression that should be compared to $\tan \alpha_i$. But, once higher order terms matter, Monge parametrization not only becomes technically impenetrable, it is even incapable of dealing with membrane shapes that display overhangs. It is hence preferable to discard it in favor of a more general numerical surface triangulation.

Reynwar and Deserno [267] have studied the interaction problem for identical axisymmetric colloids with large angles α_i, using the package "Surface Evolver" by Brakke [281]. For small angles α_i, the large distance predictions coincide well with Eq. (18), but they break down rather abruptly as soon as $r < 2r_0$, which is when the particles would touch unless they could also tilt out of each other's way. For large α_i, the linear predictions substantially overestimate the repulsion. Interestingly, for the special case $\alpha = \pi/2$ the repulsive force goes through a maximum (around $r/r_0 \approx 1.8$), and it decreases upon moving the particles even close together until it vanishes at $r/r_0 \approx 1$. At even closer distances the particles attract. Attractive forces must also exist for detachment angles smaller than $\pi/2$, but Reynwar and Deserno [267] do not attempt to find the minimal angle at which this happens. Attractive forces certainly also exist for angles bigger than $\pi/2$, even though it might be that there is also a largest angle for which they exist. In any case, only for $\alpha = \pi/2$ does the attraction persist all the way to $r = 0$.

A simple close distance approximation can be devised to understand the necessity of a sign-flip. At sufficiently close distances, the two particles tilt so much that

they almost face each other and the membrane between them assumes a shape similar to a cylinder, which is capable of transmitting tensile forces as we have seen in Sect. 2.3. For angles close to $\pi/2$, this theory suggests [267]:

$$\frac{Fr_0}{\pi\kappa} = \frac{1}{x^2} + \frac{1-\sin\alpha}{x} - 1 + \mathcal{O}(x) \qquad \text{with} \quad x = \frac{r}{2r_0\cos\alpha} \ . \tag{23}$$

Observe that the first two terms vanish for $\alpha = \pi/2$, which leaves the (attractive) force $F = \pi\kappa/r_0$, which is half the value transmitted through a cylindrical membrane tube [see Eq. (5)]. The missing factor of 2 derives from the fact that this calculation is not made at constant area but at constant (in fact, zero) tension. The numerical calculations suggest that indeed $F(r)$ approaches a constant as $r \to 0$, even though it seems slightly off from the expected value of $-\pi\kappa/r_0$.

3.2.8 Curvature-Mediated Interactions in Simulations

The experiments by Koltover et al. claim that isotropic colloids on membranes experience a surface-mediated (presumably, curvature-mediated) attraction. All theories we have discussed so far claim that the force is repulsive, unless one goes to large detachment angles. Can simulations shed more light onto the problem? If so, it will not be necessary to represent the bilayer in any greater detail because only fluid curvature elasticity needs to be captured.

Reynwar et al. have investigated this problem using the Cooke model, amended by simple generic particles with some given isotropic curvature [282]. They showed that indeed strongly membrane-deforming colloids experience attractive pair interactions. Subsequent more detailed studies revealed that these are compatible with the numerical results discussed in the previous section [267]. However, they also showed that a large number of weakly membrane deforming colloids still aggregate, in fact, that they can drive vesiculation of the membrane [282]. This is surprising because these particles exhibited detachment angles at which the ground state theory clearly insists on a repulsive pair potential.

However, just because the pair potentials are repulsive does not yet prove that aggregation cannot happen, since curvature-mediated interactions are not pairwise additive, as first pointed out by Kim et al. [283, 284]. These authors provide a general formula for an N-body interaction, and even though it is really only accurate up to the triplet level [269], it does show that the contributions beyond pairs can lower the overall repulsive energy; for instance, they show that certain multiparticle configurations are indeed marginally stable instead of being driven apart. In a later publication, Kim et al. [285] show that an infinite number of periodic lattices exist for which summing the non-pairwise interactions preserve zero membrane bending energy. Again, because their non-pairwise form is only accurate up to triplet order, it is not clear whether this result remains true if all orders are considered. Müller and Deserno have alternatively treated this problem using a cell model [286] in which a regular lattice of particles is replaced by a single particle within a cell, plus

boundary conditions that mimic the presence of other surrounding particles. They prove that within this approximation the lateral pressure between colloids is always repulsive, even in the nonlinear regime;[6] however, how well the cell model actually captures a multiparticle assembly is difficult to say. Auth and Gompper have also used a cell model approach [287], but they specifically apply it to a curved background membrane. They argue that even if the forces are repulsive, they might be less repulsive, and thus the free energy per colloid smaller, if the background membrane is curved because this background curvature screens the repulsion between the colloids. This could provide a driving force for creating curved vesicle buds from flat membranes studded with isotropic membrane-curving colloids, provided the average area density of colloids remains fixed. The latter is usually the case in simulations, and Auth and Gompper show that the sizes of the vesicles that detach from the parent membrane for differently curved colloids are compatible with the observations of Reynwar et al. [282]. What would fix this density in real systems is less clear, but it is conceivable that this is yet another situation where rafts come into play. If the membrane-curving particles have to stay within a finite raft, their mutual repulsion can, by virtue of the mechanism discussed by Auth and Gompper, lead to a budding of that raft domain.

In conclusion, we see that the situation is substantially more tricky than the seemingly simple question "do membrane-curving particles attract or repel?" leads one to expect. Nonlinearities, multibody interactions, fluctuations, background curvature, boundary conditions, and anisotropies are only some of the "details" that affect the answer to this question. At the moment, the situation remains not completely solved, but the results outlined in this section should provide a reliable guide for future work.

4 Multiscale Modeling of Lipid and Membrane Protein Systems

4.1 Multiscale Modeling: Approaches and Challenges

As we have seen in the previous sections, coarse-grained lipid models have been enormously successful for investigating phenomena in lipid bilayers and lipid bilayer/protein systems. In particular, rather coarse, generic models that reduce the lipids to their most essential features and shed almost all chemical specificity have contributed enormously to our understanding of effective interactions, generalized processes, and their driving forces. A different branch of coarse-grained models, the bottom-up models, has also progressed quite dramatically in the past

[6] They used the same techniques that also led to the exact Eq. (14), only that in the cell model case the sign is evident from the expression.

decade. These models have not been developed as stand-alone models with parameters derived to reproduce some desired experimentally known feature of the system. They were developed in a bottom-up way with the help of an underlying higher-resolution (atomistic) model. Therefore, the terms "multiscale modeling" or "systematic coarse graining" are frequently used. These models allow staying closer to an atomistic system and to retain more chemical specificity. Due to their bottom-up construction, they offer the opportunity to go back and forth between a coarse-grained and an atomistic level of resolution using so-called backmapping techniques.

It should be noted that this closeness between levels of resolution does come at a cost: upon reducing the number of degrees of freedom, the models become strongly state-point dependent and it necessarily becomes impossible to accurately represent all properties of the underlying atomistic system with the coarse-grained model. In particular, the representation of thermodynamic and structural properties is a severe challenge that has been subject of a multitude of studies over the last few years [288]. The question of representability and the unavoidable choice of parametrization target properties that has to be made has led to a number of different systematic coarse graining approaches, which are often divided into two general categories: (i) methods where the CG parameters are refined so that the system displays a certain thermodynamic behavior (typically termed "thermodynamics-based") [83, 84, 289 291] or (ii) methods where the CG system aims at reproducing the configurational phase space sampled by an atomistic reference system (often misleadingly termed "structure-based") [58, 59, 64, 292 301]. Representability limitations lead to the observation that a structure-based approach does not necessarily yield correct thermodynamic properties such as solvation free energies or partitioning data, whereas thermodynamics-based potentials may not reproduce microscopic structural data such as the local packing or the structure of solvation shells. Closely related are also the inevitable transferability problems of CG models: all CG models (in fact also all classical atomistic force fields) are state-point dependent and cannot necessarily (without reparametrization) be transferred to different thermodynamic conditions (temperature, density, concentration, system composition, phase, etc.) or to a different chemical or molecular environment (e.g., a certain chemical unit being part of different macromolecular chains). Structural and thermodynamic representability and state-point transferability questions are often intimately linked because the response to a change in state point corresponds to representing certain thermodynamic properties. Intensive research is currently devoted to this problem [299, 300, 302 308] because an understanding of the potential and limitations of coarse-grained models is a necessary prerequisite to applying them to complex biomolecular problems and systems such as multiprotein complexes in biomembranes. The reason for this is that CG models are usually developed based on smaller and less complex reference systems a reference simulation of the actual target system is by construction prohibitive, otherwise the whole coarse-graining effort would not be necessary in the first place. Consequently, it is essential to understand transferability among different concentrations,

compositions, and environments to be able to put these subsystem-based models together and obtain a reliable model for the actual, more complex, target system. We will show for one example the light-harvesting complex of green plants (LHCII) some aspects of multiscale modeling of membrane protein systems and some of the problems that need to be addressed if one wants to go beyond generic CG models and retain a certain level of chemical specificity.

4.2 The Light-Harvesting Complex

The major light-harvesting complex (LHCII) of the photosynthetic apparatus in green plants binds more than half of the plant's chlorophyll (Chl) and is presumably the most abundant membrane protein on Earth. It has become an intensely studied model membrane protein for several reasons. Its structure is known in near-atomic detail [309, 310] and much of its biochemistry has been elaborated in the past decades [311]. Moreover, LHCII spontaneously self-organizes from its protein and pigment components in vitro; therefore, recombinant versions of it can easily be produced and modified almost at will [312]. The assembly of LHCII and the concomitant folding of its apoprotein has been studied in some detail [313, 314]. Both processes occur spontaneously upon combining the unfolded apoprotein and pigments in detergent solution. In vivo, the assembly of LHCII takes place in the lipid environment of the thylakoid membrane and, most likely, is influenced by the lipid and protein components of this membrane. This is difficult to analyze experimentally because, so far, the self-organization of LHCII cannot yet be achieved in a lipid membrane environment. Recently, the disassembly of LHCII and the role of the bound/dissociating pigments in the falling apart of LHCII trimers has also become the subject of increased interest. These pigments constitute about one third of the total mass of LHCII and, according to the structure, significantly contribute to the stability of the pigment protein complex. The structural behavior of LHCII has been analyzed by circular dichroism (CD), fluorescence, and electron paramagnetic resonance (EPR) [312, 314 316].

One important aspect of LHCII that specifically relates to other aspects discussed in the present review is the question of how the membrane environment (lipid composition, membrane curvature, etc.) affects the association of LHCII monomers to form trimers and the assembly of these trimers into the antenna complex around the photosynthetic reaction centers. The nonbilayer-forming lipid monogalactosyldiacylglycerol (MGDG) constitutes half of the thylakoid membrane. This membrane maintains its lamellar structure only with proteins inserted, predominantly LHCII which, due to its concave shape, eases the curvature pressure exerted by MGDG. It has been suggested that this curvature pressure is a driving force for protein interaction in the membrane [317]; however, because it is not known whether, e.g., the formation of supercomplexes of LHCII trimers eases or increases curvature pressure, it is unclear whether MGDG (or other curvature

pressure-increasing lipid components) promote or inhibit the formation of such supercomplexes. Likewise, the composition of the lipid membrane and the membrane properties such as its curvature pressure most likely influence the folding of the LHCII apoprotein and its assembly with pigments.

LHCII commends itself as a useful model for studying the influence of the lipid membrane on the assembly and structural behavior of membrane proteins in general because of its known structure, its availability in a recombinant form, and its self-organization, at least in detergent micelles. Moreover, the bound Chl molecules serve as built-in fluorescence markers for monitoring the structural behavior of the pigment protein complex. To be able to correlate experimental observations of aggregate formation with predictions from theory, recombinant LHCII has been inserted in liposomes and assayed for complex complex distances by intercomplex FRET measurements, and for aggregate formation by quantifying aggregate-induced fluorescence quenching.

A multiscale simulation model to study the LHCII complex requires, as a first step, model parameters for all components involved. As already mentioned above, it will be neither possible nor useful to parameterize a CG model based on the actual multicomponent (lipid bilayer/protein/pigments) system but one would rather develop models for sensibly chosen subsystems. Although parameters for the protein and the lipid bilayer can typically be found in many standard force fields, a challenging first task is to obtain a reliable model for the pigments, irrespective of the level of resolution. For many biological applications, the MARTINI CG force field (described above) has become very popular and successful, in particular for lipid bilayer and protein systems. To employ the MARTINI force field for simulations of the pigmented LHCII, a CG description and model parameters for the pigment molecules needs to be added. We have developed a coarse-grained model of the chlorophyll pigments (Chl*b* and Chl*a*) that can be embedded into the existing MARTINI force field to study the pigmented LHCII trimer in the future. To do this, Chl*b* and Chl*a* were parameterized in the presence of the lipid bilayer. This reference system for parametrization was chosen for two reasons: most importantly, the Chl lipid interactions are highly relevant for the formation and behavior of the LHCII protein pigment complex in the lipid bilayer. About 50% of the pigment molecules in the plant are bound to the light-harvesting complex, with 42 Chl molecules per LHCII trimer. In vitro studies have shown that the folding of the LHCII apoprotein and the pigment binding to the protein are tightly coupled processes. In the LHCII monomer, many Chl pigments are situated in the outer region of the protein, effectively forming an interface between protein and lipids. Consequently, the Chl lipid interactions are probably important for the assembly and stability of the trimer. A second reason for choosing the Chl lipid system as reference for which the interactions between the MARTINI standard forcefield and Chl can be tuned is that it is more tractable compared to the fully pigmented LHCII membrane protein complex. The CG model for Chl*b* and Chl*a* in the DPPC bilayer was derived from a combination of a structure-based approach for bonded interaction potentials and a mixed structure-based and partitioning-based approach for

nonbonded interaction potentials to fit the thermodynamics-based MARTINI force field. The CG model for Chl molecules follows the degree of coarse graining of the MARTINI force field. Somewhat in line with the general MARTINI parameterization philosophy, which focuses on partitioning properties, the nonbonded parameters were chosen such that the distribution of the CG Chl beads between hydrophilic and hydrophobic regions in the bilayer is correctly represented, as compared to the atomistic reference simulation. Here, particular attention was paid to the interactions of the polar center of the porphyrin ring with the lipid beads and to the polarity of the aromatic ring, which needs to be carefully tuned to obtain the correct distribution between the polar headgroup and the hydrophobic tail regions of the lipid bilayer. The bonded interactions in the CG pigments were derived such that the CG model reproduces the shape and the conformational behavior of the atomistic Chl molecules. The overall shape of the porphyrin ring and the different conformations of the phytol tail are well represented in this CG model. As a last aspect of validation of the CG model, we have analyzed the propensity of the Chl pigments to aggregate in the lipid bilayer. It was found that Chl molecules do aggregate, with clusters that form and break multiple times in the course of the simulation, i.e., the aggregation is not overly strong. Qualitatively, these data are corroborated by fluorescence quenching experiments that show that chlorophylls in lipid bilayers have a tendency to aggregate at low lipid to Chl ratios of less than 1,250 lipids/chlorophyll. Summarizing the structural behavior, the distribution of the pigments in the bilayer (which are indicative of a correct balance of hydrophobicity and hydrophilicity) and the pigment association are very well represented in the CG model compared to atomistic simulations and experimental data (Debnath et al., unpublished data).

After driving the CG model parameters for the Chl lipid system, this new model was now combined with the MARTINI model for proteins to perform some first simulations of the pigmented LHCII complex (in trimeric as well as monomeric form). In addition, classical atomistic (explicit solvent) simulations of trimeric and monomeric LHCII in a model membrane were performed to provide a reference for validation of the CG simulations. The first CG simulations of the LHCII complex have proven to be very promising. Unlike our initial attempts without the careful parameterization of the pigments, the trimeric protein pigment complex has been structurally stable, most notably without the presence of any artificial elastic network between the protein core and the pigments (see Fig. 3). The properties of the complex from the CG model are in excellent agreement with those from the atomistic model. In the future, this CG model will be used to study various aspects of LHCII protein protein interactions in the lipid bilayer that, on the one hand, go beyond the time and length scales accessible to atomistic simulations alone and, on the other hand, require a more chemically realistic description of the protein/pigment/lipid system than typical generic CG models.

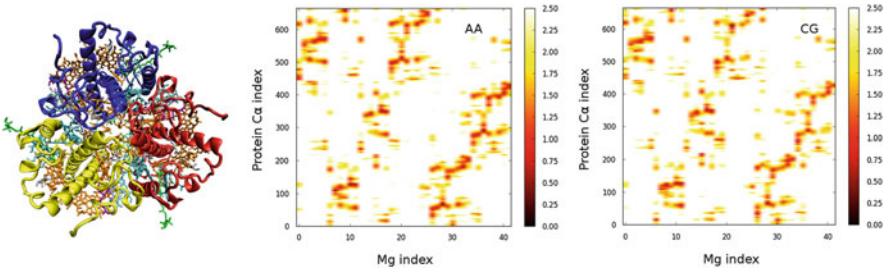

Fig. 3 *Left*: Top view of an LHCII trimer (colors according to chain or molecule type: *blue* chain A, *red* chain B, *green* chain C, *cyan* Chl*b*, *pink* Chl*a*). *Middle and right*: Contact maps between Chl pigments and protein residues of LHCII trimer drawn as distance maps between the Cα atoms of the proteins (*y* axis) and the Mg atoms of all Chl pigments (*x* axis) within a 2.5 nm cut off for atomistic (*AA*) simulations of 70 ns (*middle*) and coarse grained (*CG*) simulations of 100 ns (*right*). The maps show that the pigments are stably located in their binding sites for both levels of resolution

5 Conclusions

In this chapter we have presented an overview of different approaches to the study of lipid membranes and membrane protein systems. We have reviewed theoretical and simulation approaches, and shown how generic lipid simulation models can be used to understand the principles that determine properties of lipid bilayers such as bending, Gaussian curvature modulus, and membrane tension, or fundamental phenomena such as the formation of lipid rafts or the curvature-mediated interactions between proteins. In the previous section it was outlined how multiscale modeling can in principle go a step further by ensuring a certain chemical specificity while still benefiting from the time- and length-scale advantages of coarse-grained simulations. It was noted that there are still a number of challenges in the area of systematic coarse graining that need to be addressed to be able to study complex multicomponent systems such as the light-harvesting complex of green plants. For this system, we have shown the first steps toward a multiscale simulation model that allows going back and forth between a coarse-grained and an atomistic level of resolution and therefore permits immediate comparison to atomic level experimental data.

Acknowledgements We would like to thank the many coworkers and colleagues who have contributed to the research reported here, in particular Ira Cooke, Jemal Guven, Vagelis Harmandaris, Gregoria Illya, Martin Müller, Benedict Reynwar, Ira Rothstein, Cem Yolcu, Frank Brown, Olaf Lenz, Sebastian Meinhardt, Peter Nielaba, Beate West, Ananya Debnath, Christoph Globisch, Christoph Junghans, Shahoua Ding, Sabine Wiegand, Sandra Ritz, and Eva Sinner.

References

1. Smith R, Tanford C (1972) The critical micelle concentration of L_α dipalmitoylphosphati dylcholine in water and water/methanol solutions. J Mol Biol 67(1):75 83
2. Israelachvili JN, Mitchell DJ, Ninham BW (1976) Theory of self assembly of hydrocarbon amphiphiles into micelles and bilayers. J Chem Soc Faraday Trans 72(2):1525 1568
3. Rawicz W, Olbrich K, McIntosh T, Needham D, Evans E (2000) Effect of chain length and unsaturation on elasticity of lipid bilayers. Biophys J 79:328 339
4. Canham PB (1970) The minimum energy of bending as a possible explanation of the biconcave shape of the human red blood cell. J Theoret Biol 26(1):61 81
5. Helfrich W (1973) Elastic properties of lipid bilayers theory and possible experiments. Z Naturforsch C 28(11):693 703
6. Evans EA (1974) Bending resistance and chemically induced moments in membrane bila yers. Biophys J 14(12):923 931
7. Helfrich W (1974) The size of bilayer vesicles generated by sonication. Phys Lett A 50 (2):115 116
8. Kreyszig E (1991) Differential geometry. Dover, New York
9. do Carmo M (1976) Differential geometry of curves and surfaces. Prentice Hall, Englewood Cliffs
10. Lipowsky R, Grotehans S (1993) Hydration versus protrusion forces between lipid bilayers. Europhys Lett 23:599 604
11. Lipowsky R, Grotehans S (1993) Renormalization of hydration forces by collective protru sion modes. Biophys Chem 49:27 37
12. Goetz R, Gompper G, Lipowsky R (1999) Mobility and elasticity of self assembled mem branes. Phys Rev Lett 82:221 224
13. Brandt EG, Edholm O (2010) Stretched exponential dynamics in lipid bilayer simulations. J Chem Phys 133:115101
14. Brandt EG, Braun AR, Sachs JN, Nagle JF, Edholm O (2011) Interpretation of fluctuation spectra in lipid bilayer simulations. Biophys J 100:2104 2111
15. Lindahl E, Edholm O (2000) Mesoscopic undulations and thickness fluctuations in lipid bilayers from molecular dynamics simulations. Biophys J 79(1):426 433
16. Owicki JC, Springgate MW, McConnell HM (1978) Theoretical study of protein lipid interactions in bilayer membranes. Proc Natl Acad Sci USA 75:1616 1619
17. Owicki JC, McConnell HM (1979) Theory of protein lipid and protein protein interactions in bilayer membranes. Proc Natl Acad Sci USA 76:4750 4754
18. Huang HW (1986) Deformation free energy of bilayer membrane and its effect on gramicidin channel lifetime. Biophys J 50:1061 1070
19. Sperotto MM, Mouritsen OG (1991) Monte Carlo simulation of lipid order parameter profiles near integral membrane proteins. Biophys J 59:261 270
20. Dan N, Pincus P, Safran SA (1993) Membrane induced interactions between inclusions. Langmuir 9:2768 2771
21. Dan N, Berman A, Pincus P, Safran SA (1994) Membrane induced interactions between inclusions. J Phys II (France) 4:1713
22. Aranda Espinoza H, Berman A, Dan N, Pincus P, Safran S (1996) Interaction between inclusions embedded in membranes. Biophys J 71:648
23. Huang HW (1995) Elasticity of lipid bilayer interacting with amphiphilic helical peptides. J Phys II (France) 5:1427 1431
24. Nielsen C, Goulian M, Andersen OS (2000) Energetics of inclusion induced bilayer defor mations. Biophys J 74:1966 1983
25. Harroun TA, Heller WT, Weiss TM, Yang L, Huang HW (1999) Theoretical analysis of hydrophobic matching and membrane mediated interactions in lipid bilayers containing gramicidin. Biophys J 76:3176 3185

26. Nielsen C, Andersen OS (2000) Inclusion induced bilayer deformations: effects of mono layer equilibrium curvature. Biophys J 79:2583 2604
27. Jensen MO, Mouritsen OG (2004) Lipids do influence protein function the hydrophobic matching hypothesis revisited. Biochim Biophys Acta 1666:205 226
28. Brannigan G, Brown F (2006) A consistent model for thermal fluctuations and protein induced deformations in lipid bilayer. Biophys J 90:1501
29. Brannigan G, Brown FLH (2007) Contributions of Gaussian curvature and nonconstant lipid volume to protein deformation of lipid bilayers. Biophys J 92:864 876
30. West B, Brown FLH, Schmid F (2009) Membrane protein interactions in a generic coarse grained model for lipid bilayers. Biophys J 96:101 115
31. Fournier JB (1998) Coupling between membrane tilt difference and dilation: a new "ripple" instability and multiple crystalline inclusions phases. Europhys Lett 43:725 730
32. Fournier JB (1999) Microscopic membrane elasticity and interactions among membrane inclusions: interplay between the shape, dilation, tilt and tilt difference modes. Eur Phys J B 11:261 272
33. Bohinc K, Kralj Iglic V, May S (2003) Interaction between two cylindrical inclusions in a symmetric lipid bilayer. J Chem Phys 119:7435 7444
34. May ER, Narang A, Kopelevich DI (2007) Role of molecular tilt in thermal fluctuations of lipid membranes. Phys Rev E 76:021913
35. Watson MC, Penev ES, Welch PM, Brown FLH (2011) Thermal fluctuations in shape, thickness, and molecular orientation in lipid bilayers. J Chem Phys 135:244701
36. Watson MC, Morriss Andrews A, Welch PM, Brown FLH (2013) Thermal fluctuations in shape, thickness, and molecular orientation in lipid bilayers II: finite surface tensions. J Chem Phys 139:084706 doi: 10.1063/1.4818530
37. Neder J, West B, Nielaba P, Schmid F (2010) Coarse grained simulations of membranes under tension. J Chem Phys 132:115101
38. Li J, Pastor KA, Shi AC, Schmid F, Zhou J (2013) Elastic properties and line tension of self assembled bilayer membranes. Phys Rev E 88:012718 doi: 10.1103/PhysRevE.88.012718
39. Scott H (2002) Modeling the lipid component of membranes. Curr Opin Struct Biol 12(4): 495 502
40. Saiz L, Bandyopadhyay S, Klein ML (2002) Towards an understanding of complex biolog ical membranes from atomistic molecular dynamics simulations. Biosci Rep 22(2):151 173
41. Saiz L, Klein ML (2002) Computer simulation studies of model biological membranes. Acc Chem Res 35(6):482 489
42. Berkowitz ML (2009) Detailed molecular dynamics simulations of model biological mem branes containing cholesterol. Biochim Biophys Acta Biomembr 1788(1):86 96
43. Niemelä PS, Hyvonen MT, Vattulainen I (2009) Atom scale molecular interactions in lipid raft mixtures. Biochim Biophys Acta 1788(1):122 135
44. Gompper G, Kroll DM (1997) Network models of fluid, hexatic and polymerized membranes. J Phys Condens Matt 9(42):8795 8834
45. Gompper G, Kroll D (1998) Membranes with fluctuating topology: Monte Carlo simulations. Phys Rev Lett 81(11):2284 2287
46. Kumar PBS, Gompper G, Lipowsky R (2001) Budding dynamics of multicomponent mem branes. Phys Rev Lett 86(17):3911 3914
47. Noguchi H, Gompper G (2004) Fluid vesicles with viscous membranes in shear flow. Phys Rev Lett 93(25):258102
48. Atzberger PJ, Kramer PR, Peskin CS (2007) A stochastic immersed boundary method for fluid structure dynamics at microscopic length scales. J Comput Phys 224(2):1255 1292
49. Brown FLH (2008) Elastic Modeling of biomembranes and lipid bilayers. Ann Rev Phys Chem 59:685 712
50. Venturoli M, Sperotto MM, Kranenburg M, Smit B (2006) Mesoscopic models of biological membranes. Phys Rep 437(1 2):1 54
51. Müller M, Katsov K, Schick M (2006) Biological and synthetic membranes: what can be learned from a coarse grained description? Phys Rep 434(5 6):113 176

52. Brannigan G, Lin L, Brown F (2006) Implicit solvent simulation models for biomembranes. Eur Biophys J 35(2):104 124
53. Marrink Siewert J, de Vries AH, Tieleman DP (2009) Lipids on the move: simulations of membrane pores, domains, stalks and curves. Biochim Biophys Acta Biomembr 1788 (1):149 168
54. Bennun SV, Hoopes MI, Xing C, Faller R (2009) Coarse grained modeling of lipids. Chem Phys Lipids 159(2):59 66
55. Deserno M (2009) Mesoscopic membrane physics: concepts, simulations, and selected applications. Macromol Rapid Comm 30(9 10):752 771
56. Noguchi H (2009) Membrane simulation models from nanometer to micrometer scale. J Phys Soc Jpn 78(4):041007
57. Schmid F (2009) Toy amphiphiles on the computer: What can we learn from generic models? Macromol Rapid Comm 30:741 751
58. Müller Plathe F (2002) Coarse graining in polymer simulation: from the atomistic to the mesoscopic scale and back. Chem Phys Chem 3(9):754 769
59. Izvekov S, Both GA (2005) Multiscale coarse graining of liquid state systems. J Chem Phys 123(13):134105
60. Praprotnik M, Delle Site L, Kremer K (2005) Adaptive resolution molecular dynamics simulation: changing the degrees of freedom on the fly. J Chem Phys 123(22):224106
61. Praprotnik M, Delle Site L, Kremer K (2007) A macromolecule in a solvent: adaptive resolution molecular dynamics simulation. J Chem Phys 126(13):134902
62. Praprotnik M, Site LD, Kremer K (2008) Multiscale simulation of soft matter: from scale bridging to adaptive resolution. Ann Rev Phys Chem 59(1):545 571
63. Delgado Buscalioni R, Kremer K, Praprotnik M (2008) Concurrent triple scale simulation of molecular liquids. J Chem Phys 128(11):114110
64. Noid WG, Chu JW, Ayton GS, Krishna V, Izvekov S, Voth GA, Das A, Andersen HC (2008) The multiscale coarse graining method. I. A rigorous bridge between atomistic and coarse grained models. J Chem Phys 128(24):244114
65. Noid WG, Liu P, Wang Y, Chu JW, Ayton GS, Izvekov S, Andersen HC, Voth GA (2008) The multiscale coarse graining method. II. Numerical implementation for coarse grained molecular models. J Chem Phys 128(24):244115
66. Das A, Andersen HC (2009) The multiscale coarse graining method. III. A test of pairwise additivity of the coarse grained potential and of new basis functions for the variational calculation. J Chem Phys 131(3):034102
67. Delgado Buscalioni R, Kremer K, Praprotnik M (2009) Coupling atomistic and continuum hydrodynamics through a mesoscopic model: application to liquid water. J Chem Phys 131(24):244107
68. Peter C, Kremer K (2009) Multiscale simulation of soft matter systems from the atomistic to the coarse grained level and back. Soft Matter 5:4357 4366
69. Poblete S, Praprotnik M, Kremer K, Delle Site L (2010) Coupling different levels of resolution in molecular simulations. J Chem Phys 132(11):114101
70. Voth GA (ed) (2008) Coarse graining of condensed phase and biomolecular systems, 1st edn. CRC, Boca Raton
71. Rühle V, Junghans C, Lukyanov A, Kremer K, Andrienko D (2009) Versatile object oriented toolkit for coarse graining applications. J Chem Theory Comput 5(12):3211 3223
72. Lu L, Voth GA (2012) The multiscale coarse graining method. In: Rice SA, Dinner AR (eds) Advances in chemical physics, vol 149. Wiley, Hoboken, pp 47 81 doi: 10.1002/9781118180396.ch2
73. Cooke IR, Kremer K, Deserno M (2005) Tunable generic model for fluid bilayer membranes. Phys Rev E 72(1):011506
74. Cooke IR, Deserno M (2005) Solvent free model for self assembling fluid bilayer mem branes: stabilization of the fluid phase based on broad attractive tail potentials. J Chem Phys 123(22):224710

75. Cooke IR, Deserno M (2006) Coupling between lipid shape and membrane curvature. Biophys J 91(2):487 495
76. Hu M, Briguglio JJ, Deserno M (2012) Determining the Gaussian curvature modulus of lipid membranes in simulations. Biophys J 102(6):1403 1410
77. Schmid F, Düchs D, Lenz O, West B (2007) A generic model for lipid monolayers, bilayers, and membranes. Comp Phys Comm 177(1 2):168
78. Düchs D, Schmid F (2001) Phase behavior of amphiphilic monolayers: theory and simula tions. J Phys Cond Matt 13:4853
79. Lenz O, Schmid F (2005) A simple computer model for liquid lipid bilayers. J Mol Liquid 117(1 3):147 152
80. Lenz O, Schmid F (2007) Structure of symmetric and asymmetric ripple phases in lipid bilayers. Phys Rev Lett 98:058104
81. Meinhardt S, Vink R, Schmid F (2013) Monolayer curvature stabilizes nanoscale raft domains in mixed lipid bilayers. Proc Natl Acad Sci USA 12:4476 4481
82. Pike L (2006) Rafts defined: a report on the keystone symposium on lipid rafts and cell function. J Lipid Res 47:1597 1598
83. Marrink SJ, de Vries AH, Mark AE (2004) Coarse grained model for semiquantitative lipid simulations. J Phys Chem B 108(2):750 760
84. Marrink SJ, Risselada HJ, Yefimov S, Tieleman DP, de Vries AH (2007) The MARTINI force field: coarse grained model for biomolecular simulations. J Phys Chem B 111:7812 7824
85. Monticelli L, Kandasamy SK, Periole X, Larson RG, Tieleman DP, Marrink SJ (2008) The MARTINI coarse grained force field: extension to proteins. J Chem Theory Comput 4(5):819 834
86. López CA, Rzepiela AJ, de Vries AH, Dijkhuizen L, Huenenberger PH, Marrink SJ (2009) Martini coarse grained force field: extension to carbohydrates. J Chem Theory Comput 5(12):3195 3210
87. López EA, Sovova Z, van Eerden FJ, de Vries AH, Marrink SJ (2013) MARTINI force field parameters for glycolipids. J Chem Theory Comput 9(3):1694 1708
88. Lee S (1962) Spiderman, Amazing fantasy # 15. Marvel Comics, New York
89. Brochard F, Lennon JF (1975) Frequency spectrum of flicker phenomenon in erythrocytes. J Phys (France) 36(11):1035 1047
90. Brochard F, De Gennes PG, Pfeuty P (1976) Surface tension and deformations of membrane structures: relation to two dimensional phase transitions. J Phys (France) 37:1099
91. Schneider MB, Jenkins JT, Webb WW (1984) Thermal fluctuations of large cylindrical phospholipid vesicles. Biophys J 45(5):891 899
92. Schneider MB, Jenkins JT, Webb WW (1984) Thermal fluctuations of large quasi spherical bimolecular phospholipid vesicles. Biophys J 45(9):1457 1472
93. Faucon JF, Mitov MD, Méléard P, Bivas I, Bothorel P (1989) Bending elasticity and thermal fluctuations of lipid membranes theoretical and experimental requirements. J Phys (France) 50(17):2389 2414
94. Henriksen J, Rowat AC, Ipsen JH (2004) Vesicle fluctuation analysis of the effects of sterols on membrane bending rigidity. Eur Biophys J 33(8):732 741
95. Evans E, Rawicz W (1990) Entropy driven tension and bending elasticity in condensed fluid membranes. Phys Rev Lett 64(17):2094 2097
96. Liu YF, Nagle JF (2004) Diffuse scattering provides material parameters and electron density profiles of biomembranes. Phys Rev E 69(4):040901
97. Chu N, Kučerka N, Liu YF, Tristram Nagle S, Nagle JF (2005) Anomalous swelling of lipid bilayer stacks is caused by softening of the bending modulus. Phys Rev E 71(4):041904
98. Tristram Nagle S, Nagle JF (2007) HIV 1 fusion peptide decreases bending energy and promotes curved fusion intermediates. Biophys J 93(6):2048 2055
99. Pan J, Tristram Nagle S, Kučerka N, Nagle JF (2008) Temperature dependence of structure, bending rigidity, and bilayer interactions of dioleoylphosphatidylcholine bilayers. Biophys J 94(1):117 124

100. Pfeiffer W, König S, Legrand JF, Bayerl T, Richter D, Sackmann E (1993) Neutron spin echo study of membrane undulations in lipid multibilayers. Europhys Lett 23(6):457 462
101. Takeda T, Kawabata Y, Seto H, Komura S, Ghosh SK, Nagao M, Okuhara D (1999) Neutron spin echo investigations of membrane undulations in complex fluids involving amphiphiles. J Phys Chem Solids 60(8 9):1375 1377
102. Rheinstädter MC, Häußler W, Salditt T (2006) Dispersion relation of lipid membrane shape fluctuations by neutron spin echo spectrometry. Phys Rev Lett 97(4):048103
103. Watson MC, Brown FLH (2010) Interpreting membrane scattering experiments at the mesoscale: the contribution of dissipation within the bilayer. Biophys J 98(6):L09 L11
104. Bo L, Waugh RE (1989) Determination of bilayer membrane bending stiffness by tether formation from giant, thin walled vesicles. Biophys J 55(3):509 517
105. Cuvelier D, Derényi I, Bassereau P, Nassoy P (2005) Coalescence of membrane tethers: experiments, theory, and applications. Biophys J 88(4):2714 2726
106. Tian A, Baumgart T (2008) Sorting of lipids and proteins in membrane curvature gradients. Biophys J 96(7):2676 2688
107. Ayton G, Voth GA (2002) Bridging microscopic and mesoscopic simulations of lipid bilayers. Biophys J 83(6):3357 3370
108. Farago O (2003) "Water free" computer model for fluid bilayer membranes. J Chem Phys 119(1):596 605
109. Wang ZJ, Frenkel D (2005) Modeling flexible amphiphilic bilayers: a solvent free off lattice Monte Carlo study. J Chem Phys 122:234711
110. Wang ZJ, Deserno M (2010) A systematically coarse grained solvent free model for quan titative phospholipid bilayer simulation. J Phys Chem B 114(34):11207 11220
111. Shiba H, Noguchi H (2011) Estimation of the bending rigidity and spontaneous curvature of fluid membranes in simulations. Phys Rev E 84:031926
112. Watson MC, Brandt EG, Welch PM, Brown FLH (2012) Determining biomembrane bending rigidities from simulations of modest size. Phys Rev Lett 109:028102
113. Harmandaris VA, Deserno M (2006) A novel method for measuring the bending rigidity of model lipid membranes by simulating tethers. J Chem Phys 125(20):204905
114. Arkhipov A, Yin Y, Schulten K (2008) Four scale description of membrane sculpting by bar domains. Biophys J 95(6):2806 2821
115. Noguchi H (2011) Anisotropic surface tension of buckled fluid membranes. Phys Rev E 83:061919
116. Hu M, Diggins IVP, Deserno M (2013) Determining the bending modulus of a lipid membrane by simulating buckling. J Chem Phys 138:214110. doi:10.1063/1.4808077
117. Siegel DP, Kozlov MM (2004) The Gaussian curvature elastic modulus of n monomethylated dioleoylphosphatidylethanolamine: relevance to membrane fusion and lipid phase behavior. Biophys J 87(1):366 374
118. Siegel DP (2006) Determining the ratio of the Gaussian curvature and bending elastic moduli of phospholipids from Q_{II} phase unit cell dimensions. Biophys J 91(2):608 618
119. Siegel DP (2008) The Gaussian curvature elastic energy of intermediates in membrane fusion. Biophys J 95(11):5200 5215
120. Templer RH, Khoo BJ, Seddon JM (1998) Gaussian curvature modulus of an amphiphile monolayer. Langmuir 14(26):7427 7434
121. Baumgart T, Das S, Webb WW, Jenkins JT (2005) Membrane elasticity in giant vesicles with fluid phase coexistence. Biophys J 89(2):1067 1080
122. Semrau S, Idema T, Holtzer L, Schmidt T, Storm C (2008) Accurate determination of elastic parameters for multicomponent membranes. Phys Rev Lett 100(8):088101
123. Hu M, de Jong DH, Marrink SJ, Deserno M (2013) Gaussian curvature elasticity determined from global shape transformations and local stress distributions: a comparative study using the MARTINI model. Farad Discuss 161:365 382
124. Taupin C, Dvolaitzky M, Sauterey C (1975) Osmotic pressure induced pores in phospholipid vesicles. Biochemistry 14(21):4771 4775

125. Zhelev DV, Needham D (1993) Tension stabilized pores in giant vesicles determination of pore size and pore line tension. Biochim Biophys Acta 1147(1):89 104
126. Genco I, Gliozzi A, Relini A, Robello M, Scalas E (1993) Osmotic pressure induced pores in phospholipid vesicles. Biochim Biophys Acta 1149(1):10 18
127. Karatekin E, Sandre O, Guitouni H, Borghi N, Puech PH, Brochard Wyart F (2003) Cascades of transient pores in giant vesicles: line tension and transport. Biophys J 84(3):1734 1749
128. Tolpekina TV, den Otter WK, Briels WJ (2004) Simulations of stable pores in membranes: system size dependence and line tension. J Chem Phys 121(16):8014 8020
129. Wohlert J, den Otter WK, Edholm O, Briels WJ (2006) Free energy of a trans membrane pore calculated from atomistic molecular dynamics simulations. J Chem Phys 124(15):154905
130. Jiang FY, Bouret Y, Kindt JT (2004) Molecular dynamics simulations of the lipid bilayer edge. Biophys J 87(1):182 192
131. Wang ZJ, Deserno M (2010) Systematic implicit solvent coarse graining of bilayer mem branes: lipid and phase transferability of the force field. New J Phys 12:095004
132. Wang H, Hu D, Zhang P (2013) Measuring the spontaneous curvature of bilayer membranes by molecular dynamics simulations. Commun Comput Phys 13:1093 1106
133. Helfrich W (1985) Effect of thermal undulations on the rigidity of fluid membranes and interfaces. J Phys France 46(7):1263 1268
134. Peliti L, Leibler S (1985) Effects of thermal fluctuations on systems with small surface tension. Phys Rev Lett 54:1690 1693
135. Förster D (1986) On the scale dependence, due to thermal fluctuations, of the elastic properties of membranes. Phys Lett A 114(3):115 120
136. Kleinert H (1986) Thermal softening of curvature elasticity in membranes. Phys Lett A 114(5):263 268
137. Schmid F (2013) Fluctuations in lipid bilayers: are they understood? Biophys Rev Lett 8:1 20 doi:10.1142/S1793048012300113
138. Nelson DR, Peliti L (1987) Fluctuations in membranes with crystalline and hexatic order. J Phys (France) 48(1):1085 1092. doi:10.1051/jphys:019870048070108500
139. Le Doussal P, Radzihovsky L (1992) Self consistent theory of polymerized membranes. Phys Rev Lett 69(8):1209 1211
140. Park JM, Lubensky TC (1995) Topological defects on fluctuating surfaces: general properties and the Kosterlitz Thouless transition. Phys Rev E 53(3):2648 2664
141. Park JM (1996) Renormalization of fluctuating tilted hexatic membranes. Phys Rev E 56(7): R47 R50
142. West B, Schmid F (2010) Fluctuations and elastic properties of lipid membranes in the fluid and gel state: a coarse grained Monte Carlo study. Soft Matter 6:1275 1280
143. Kramer L (1971) Theory of light scattering from fluctuations of membranes and monolayers. J Chem Phys 55:2097 2105
144. Seifert U, Langer SA (1993) Viscous modes of fluid bilayer membranes. Europhys Lett 23(1):71 76
145. Zilman AG, Granek R (1996) Undulations and dynamic structure factor of membranes. Phys Rev Lett 77:4788 4791
146. Fromherz P (1983) Lipid vesicle structure: size control by edge active agents. Chem Phys Lett 94:259 266
147. van Kampen NG (2007) Stochastic processes in physics and chemistry, 3rd edn. Elsevier, Amsterdam
148. Helfrich W (1981) Physics of defects. North Holland, Amsterdam
149. Helfrich W (1994) Lyotropic lamellar phases. J Phys Condens Matter 6:A79 A92
150. Szleifer I, Kramer D, Ben Shaul A, Gelbart WM, Safran SA (1990) Molecular theory of curvature elasticity in surfactant films. J Chem Phys 92:6800 6817
151. Rowlinson JS, Widom B (2002) Molecular theory of capillarity, 1st edn. Dover, New York
152. Gompper G, Klein S (1992) Ginzburg Landau theory of aqueous surfactant solutions. J Phys II (France) 2:1725 1744

153. Diamant H (2011) Model free thermodynamics of fluid vesicles. Phys Rev E 84(6):0611203
154. Capovilla R, Guven J (2002) Stresses in lipid membranes. J Phys A Math Gen 35:6233 6247
155. Capovilla R, Guven J (2004) Stress and geometry of lipid vesicles. J Phys Condens Matter 16: S2187 S2191
156. Farago O, Pincus P (2004) Statistical mechanics of bilayer membrane with a fixed projected area. J Chem Phys 120:2934 2950
157. Guven J (2004) Membrane geometry with auxiliary variables and quadratic constraints. J Phys A Math Gen 37:L313 L319
158. Müller MM, Deserno M, Guven J (2005) Geometry of surface mediated interactions. Europhys Lett 69:482 488
159. Müller MM, Deserno M, Guven J (2005) Interface mediated interactions between particles: a geometrical approach. Phys Rev E 72:061407
160. Müller MM, Deserno M, Guven J (2007) Balancing torques in membrane mediated interac tions: exact results and numerical illustrations. Phys Rev E 76:011921. doi:10.1103/PhysRevE.76.011921
161. Deserno M, Müller MM, Guven J (2007) Contact lines for fluid surface adhesion. Phys Rev E 76:011605. doi:10.1103/PhysRevE.76.011605
162. Schmid F (2011) Are stress free membranes really "tensionless"? Europhys Lett 95:28008
163. Deuling H, Helfrich W (1976) The curvature elasticity of fluid membranes: a catalogue of vesicle shapes. J Phys (France) 37:1335 1345
164. David F, Leibler S (1991) Vanishing tension of fluctuating membranes. J Phys II (France) 1:959 976
165. Cai W, Lubensky TC, Nelson P, Powers T (1994) Measure factors, tension, and correlations of fluid membranes. J Phys II (France) 4:931 949
166. Jähnig F (1996) What is the surface tension of a lipid bilayer membrane? Biophys J 71:1348 1349
167. Marsh D (1997) Renormalization of the tension and area expansion modulus in fluid membranes. Biophys J 73:865 869
168. Farago O, Pincus P (2003) The effect of thermal fluctuations on Schulman area elasticity. Eur Phys J E 11:399 408
169. Imparato A (2006) Surface tension in bilayer membranes with fixed projected area. J Chem Phys 124:154714
170. Stecki J (2008) Balance of forces in simulated bilayers. J Phys Chem B 112(14):4246 4252
171. Fournier JB, Barbetta C (2008) Direct calculation from the stress tensor of the lateral surface tension of fluctuating fluid membranes. Phys Rev Lett 100:078103
172. Fournier JB (2012) Comment on "are stress free membranes really 'tensionless'?" by Schmid F. Europhys Lett 97:18001
173. Schmid F (2012) Reply to Comment on "are stress free membranes really 'tensionless'?". Europhys Lett 97:18002
174. Farago O (2011) Mechanical surface tension governs membrane thermal fluctuations. Phys Rev E 84:051944
175. Marrink SJ, Mark AE (2001) Effect of undulations on surface tension in simulated bilayers. J Phys Chem B 105:6122 6127
176. Loison C, Mareschal M, Kremer K, Schmid F (2003) Thermal fluctuations in a lamellar phase of a binary amphiphile solvent mixture: a molecular dynamics study. J Chem Phys 119(13): 138 13148
177. Ahmed SN, Brown DA, London E (1997) On the origin of sphingolipid/cholesterol rich detergent insoluble cell membranes: Physiological concentrations of cholesterol and sphingolipid induce formation of a detergent insoluble, liquid ordered lipid phase in model membranes. Biochemistry 36(36):10944 10953
178. Simons K, Ikonen E (1997) Functional rafts in cell membranes. Nature 387:569 572
179. Brown DA, London E (1998) Structure and origin of ordered lipid domains in biological membranes. J Membr Biol 164(2):103 114

180. Brown DA, London E (1998) Functions of lipid rafts in biological membranes. Ann Rev Cell Develop Biol 14:111 136
181. Brown DA, London E (2000) Structure and function of sphingolipid and cholesterol rich membrane rafts. J Biol Chem 275(23):17221 17224
182. Singer SJ, Nicolson GK (1972) Fluid mosaic model of structure of cell membranes. Science 175(4023):720 731
183. Munro S (2003) Lipid rafts: elusive or illusive? Cell 115(4):377 388
184. Hancock JF (2006) Lipid rafts: contentious only from simplistic standpoints. Nat Rev Mol Cell Biol 7:456 462
185. Leslie M (2011) Do lipid rafts exist? Science 334:1046 1047
186. Vereb G, Szöllosi J, Matko J, Nagy P, Farkas T, Vigh L, Matyus L, Waldmann TA, Damjanovich S (2003) Dynamic, yet structured: the cell membranes three decades after the Singer Nicolson model. Proc Natl Acad Sci USA 100:8053 8058
187. Veatch SL, Keller SL (2003) Separation of liquid phases in giant vesicles of ternary mixtures of phospholipids and cholesterol. Biophys J 85(5):3074 3083
188. Veatch SL, Keller SL (2005) Seeing spots: complex phase behavior in simple membranes. Biochim Biophys Acta 1746:172 185
189. Pralle A, Keller P, Florin EL, Simons K, Hörber JKH (2000) Sphingolipid cholesterol rafts diffuse as small entities in the plasma membrane of mammalian cells. J Cell Biol 148:997 1007
190. Turner MS, Sens P, Socci ND (2005) Nonequilibrium raft like membrane domains under continuous recycling. Phys Rev Lett 95:168301
191. Yethiraj A, Weisshaar JC (2007) Why are lipid rafts not observed in vivo? Biophys J 93:3113 3119
192. Simons K, Vaz WLC (2004) Model systems, lipid rafts, and cell membranes. Annu Rev Biophys Biomol Struct 33:269 295
193. Brewster R, Pincus PA, Safran SA (2009) Hybrid lipids as a biological surface active component. Biophys J 97:1087 1094
194. Yamamoto T, Brewster R, Safran SA (2010) Chain ordering of hybrid lipids can stabilize domains in saturated/hybrid/cholesterol lipid membranes. Europhys Lett 91:28002
195. Veatch SL, Soubias O, Keller SL, Gawrisch K (2007) Critical fluctuations in domain forming lipid mixtures. Proc Natl Acad Sci USA 104(17):650 655
196. Honerkamp Smith AR, Veatch SL, Keller SL (2009) An introduction to critical points for biophysicists: observations of compositional heterogeneity in lipid membranes. Biochim Biophys Acta 1788:53 63
197. Ipsen JH, Karlström G, Mouritsen OB, Wennerström H, Zuckermann MJ (1987) Phase equilibria in the phosphatidylcholine cholesterol system. Biochim Biophys Acta 905:162 172
198. Sankaram MB, Thompson TE (1991) Cholesterol induced fluid phase immiscibility in mem branes. Proc Natl Acad Sci USA 88:8686 8690
199. Katsaras J, Tristram Nagle S, Liu Y, Headrick RL, Fontes E, Mason PC, Nagle JF (2000) Clarification of the ripple phase of lecithin bilayers using fully hydrated, aligned samples. Phys Rev E 61:5668
200. Sengupta K, Raghunathan VA, Katsaras J (2003) Structure of the ripple phase of phospho lipid multibilayers. Phys Rev E 68(3):031710
201. Koynova R, Caffrey M (1994) Phases and phase transitions of the hydrated phosphatidyleth anolamines. Chem Phys Lipids 69:1 34
202. Koynova R, Caffrey M (1998) Phases and phase transitions of the phosphatidylcholines. Biochimica Biophysica Acta Rev Biomembr 1376:91 145
203. Kranenburg M, Smit B (2005) Phase behavior of model lipid bilayers. J Phys Chem B 109:6553 6563
204. de Vries AH, Yefimov S, Mark AE, Marrink SJ (2005) Molecular structure of the lecithin ripple phase. Proc Natl Acad Sci USA 102:5392 5396

205. Sun X, Gezelter JD (2008) Dipolar ordering in the ripple phases of molecular scale models of lipid membranes. J Phys Chem B 112:1968 1975
206. Jamroz D, Kepczynski M, Nowakowska M (2010) Molecular structure of the dioctadecyldi methylammonium bromide (DODAB) bilayer. Langmuir 26(15):076 15079
207. Chen R, Poger D, Mark AE (2011) Effect of high pressure on fully hydrated DPPC and POPC bilayers. J Phys Chem B 115:1038 1044
208. Dolezel S (2010) Computer simulation of lipid bilayers. Diploma thesis, University of Mainz
209. Brazovskii SA (1975) Phase transitions of an isotropic system to a nonuniform state. Soviet Phys JETP 41:85 89
210. Marsh D (2008) Protein modulation of lipids, and vice versa, in membranes. Biochim Biophys Acta 1778:1545 1575
211. Benjamini A, Smit B (2012) Robust driving forces for transmembrane helix packing. Biophys J 103:1227 1235
212. Cantor RS (1997) Lateral pressures in cell membranes: a mechanism for modulation of protein function. J Phys Chem B 101:1723 1725
213. Elliott J, Needham D, Dilger J, Haydon D (1983) The effects of bilayer thickness and tension on gramicidin single channel lifetimes. Biochim Biophys Acta 735:95 103
214. Botelho AV, Huber T, Sakmar TP, Brown MF (2006) Curvature and hydrophobic forces drive oligomerization and modulate activity of rhodopsin in membranes. Biophys J 91:4464 4477
215. Antonny B (2006) Membrane deformation by protein coats. Curr Opin Cell Biol 18 (4):386 394
216. Lee AG (2005) How lipids and proteins interact in a membrane: a molecular approach. Mol Biosyst 3:203 212
217. Gil T, Sabra MC, Ipsen JH, Mouritsen OG (1997) Wetting and capillary condensation as means of protein organization in membranes. Biophys J 73(4):1728 1741
218. Gil T, Ipsen JH, Mouritsen OG, Sabra MC, Sperotto MM, Zuckermann MJ (1998) Theoret ical analysis of protein organization in lipid membranes. Biochim Biophys Acta 1376 (3):245 266
219. Reynwar BJ, Deserno M (2008) Membrane composition mediated protein protein interac tions. Biointerphases 3:FA117 FA125
220. Machta BB, Veatch SL, Sethna JP (2012) Critical Casimir forces in cellular membranes. Phys Rev Lett 109:138101
221. May S, Ben Shaul A (1999) Molecular theory of lipid protein interaction and the Lalpha HII transition. Biophys J 76(2):751 767
222. May S (2000) Protein induced bilayer deformations: the lipid tilt degree of freedom. Eur Biophys J 29(1):17 28
223. Kozlovsky Y, Zimmerberg J, Kozlov MM (2004) Orientation and interaction of oblique cylindrical inclusions embedded in a lipid monolayer: a theoretical model for viral fusion peptides. Biophys J 87(2):999 1012
224. Deserno M (2009) Membrane elasticity and mediated interactions in continuum theory: a differential geometric approach. In: Faller R, Jue T, Longo ML, Risbud SH (eds) Biomembrane frontiers: nanostructures, models, and the design of life, vol 2. Springer, New York, pp 41 74
225. May S (2000) Theories on structural perturbations of lipid bilayers. Curr Opin Colloid Interface Sci 5:244 249
226. Bloom M, Evans E, Mouritsen OG (1991) Physical properties of the fluid lipid bilayer component of cell membranes: a perspective. Quart Rev Biophys 24(3):293 297
227. Killian JA (1998) Hydrophobic mismatch between proteins and lipids in membranes. Biochim Biophys Acta 1376:401 416
228. Dumas F, Lebrun MC, Tocanne JF (1999) Is the protein/lipid hydrophobic matching principle relevant to membrane organization and functions? FEBS Lett 458:271 277

229. Harroun TA, Heller WT, Weiss TM, Yang L, Huang HW (1999) Experimental evidence for hydrophobic matching and membrane mediated interactions in lipid bilayers containing gramicidin. Biophys J 76:937 945
230. De Planque MRR, Killian JA (2003) Protein lipid interactions studied with designed trans membrane peptides: role of hydrophobic matching and interfacial anchoring (review). Mol Membr Biol 20:271 284
231. Marsh D (2008) Energetics of hydrophobic matching in lipid protein interactions. Biophys J 94:3996 4013
232. Cybulski LE, de Mendoza D (2011) Bilayer hydrophobic thickness and integral membrane protein function. Curr Protein Pept Sci 12:760 766
233. Strandberg E, Esteban Martin S, Ulrich AS, Salgado J (2012) Hydrophobic mismatch of mobile transmembrane helices: merging theory and experiments. Biochim Biophys Acta 1818:1242 1249
234. Venturoli M, Smit B, Sperotto MM (2005) Simulation studies of protein induced bilayer deformations, and lipid induced protein tilting, on a mesoscopic model for lipid bilayers with embedded proteins. Biophys J 88:1778
235. Park SH, Opella SJ (2005) Tilt angle of a trans membrane helix is determined by hydropho bic mismatch. J Mol Biol 350:310 318
236. Holt A, Killian JA (2010) Orientation and dynamics of transmembrane peptides: the power of simple models. Eur Biophys J 39:609 621
237. Strandberg E, Tremouilhac P, Wadhwani P, Ulrich AS (2009) Synergistic transmembrane insertion of the heterodimeric PGLA/magainin 2 complex studied by solid state NMR. Biochim Biophys Acta 1788:1667 1679
238. Schmidt U, Weiss M (2010) Hydrophobic mismatch induced clustering as a primer for protein sorting in the secretory pathway. Biophys Chem 151:34 38
239. Harzer U, Bechinger B (2000) Alignment of lysine anchored membrane peptides under conditions of hydrophobic mismatch: A CD, ^{15}N and ^{31}P solid state NMR spectroscopy investigation. Biochemistry 39(13):106 13114
240. Özdirekcan S, Rijkers DTS, Liskamp RMJ, Killian JA (2005) Influence of flanking residues on tilt and rotation angles of transmembrane peptides in lipid bilayers. a solid state ^{2}H NMR study. Biochemistry 44:1004 1012
241. Vostrikov VV, Grant CV, Daily AE, Opella SJ, Koeppe RE II (2008) Comparison of "polarization inversion with spin exchange at magic angle" and "geometric analysis of labeled alanines" methods for transmembrane helix alignment. J Am Chem Soc 130(12): 584 12585
242. Chiang C, Shirinian L, Sukharev S (2005) Capping transmembrane helices of MscL with aromatic residues changes channel response to membrane stretch. Biochemistry 44(12): 589 12597
243. Vostrikov VV, Koeppe RE II (2011) Response of GWALP transmembrane peptides to changes in the tryptophan anchor positions. Biochemistry 50:7522 7535
244. Neder J, Nielaba P, West B, Schmid F (2012) Interactions of membranes with coarse grain proteins: a comparison. New J Phys 14:125017
245. Mouritsen OG, Bloom M (1984) Mattress model of lipid protein interactions in membranes. Biophys J 36:141 153
246. Fattal DR, Ben Shaul A (1993) A molecular model for lipid protein interaction in mem branes: the role of hydrophobic mismatch. Biophys J 65:1795 1809
247. Fattal DR, Ben Shaul A (1995) Lipid chain packing and lipid protein interaction in mem branes. Phys A 220:192 216
248. Cordomi A, Perez JJ (2007) Molecular dynamics simulations of rhodopsin in different one component lipid bilayers. J Phys Chem B 111:7052 7063
249. Neder J, West B, Nielaba P, Schmid F (2010) Membrane mediated protein protein interac tion: a Monte Carlo study. Curr Nanosci 7:656 666

250. Schmidt U, Guigas G, Weiss M (2008) Cluster formation of transmembrane proteins due to hydrophobic mismatching. Phys Rev Lett 101:128104
251. de Meyer FJM, Venturoli M, Smit B (2008) Molecular simulations of lipid mediated protein protein interactions. Biophys J 95:1851 1865
252. Koltover I, Rädler JO, Safinya CR (1999) Membrane mediated attraction and ordered aggregation of colloidal particles bound to giant phospholipid vesicles. Phys Rev Lett 82:1991 1994
253. Goulian M, Bruinsma R, Pincus P (1993) Long range forces in heterogeneous fluid mem branes. Europhys Lett 22:145
254. Goulian M, Bruinsma R, Pincus P (1993) Long range forces in heterogeneous fluid mem branes: erratum. Europhys Lett 23:155
255. Fournier JB, Dommersnes PG (1997) Comment on "long range forces in heterogeneous fluid membranes". Europhys Lett 39(6):681
256. Dommersnes P, Fournier JB (1999) N body study of anisotropic membrane inclusions: membrane mediated interactions and ordered aggregation. Eur Phys J E 12:9 12
257. Dommersnes P, Fournier J (2002) The many body problem for anisotropic membrane inclusions and the self assembly of "saddle" defects into an "egg carton". Biophys J 83:2898 2905
258. Fournier JB, Dommersnes PG, Galatola P (2003) Dynamin recruitment by clathrin coats: a physical step? C R Biol 326:467 476
259. Wu SHW, McConnell HM (1975) Phase separations in phospholipid membranes. Biochem istry 14(4):847 854
260. Gebhardt C, Gruler H, Sackmann E (1977) Domain structure and local curvature in lipid bilayers and biological membranes. Z Naturforsch C 32(7 8):581 596
261. Markin VS (1981) Lateral organization of membranes and cell shapes. Biophys J 36(1):1 19
262. Andelman D, Kawakatsu T, Kawasaki K (1992) Equilibrium shape of two component unilamellar membranes and vesicles. Europhys Lett 19(1):57 62
263. Seifert U (1993) Curvature induced lateral phase segregation in two component vesicles. Phys Rev Lett 70:1335 1338
264. Bretscher MS (1972) Asymmetrical lipid bilayer structure for biological membranes. Nature 236(61):11 12
265. Daleke DL (2007) Phospholipid flippases. J Biol Chem 282(2):821 825
266. Deserno M (2004) Elastic deformation of a fluid membrane upon colloid binding. Phys Rev E 69:031903
267. Reynwar BJ, Deserno M (2011) Membrane mediated interactions between circular particles in the strongly curved regime. Soft Matter 7:8567 8575
268. Weikl TR, Kozlov MM, Helfrich W (1998) Interaction of conical membrane inclusions: effect of lateral tension. Phys Rev E 57:6988 6995. doi:10.1103/PhysRevE.57.6988
269. Yolcu C, Deserno M (2012) Membrane mediated interactions between rigid inclusions: an effective field theory. Phys Rev E 86:031906
270. Rothstein IZ (2003) TASI lectures on effective field theories. Available from arXiv.org, ArXiv:hep ph/0308266
271. Goldberger WD, Rothstein IZ (2006) An effective field theory of gravity for extended objects. Phys Rev D 73:104029
272. Porto RA, Ross A, Rothstein IZ (2011) Spin induced multipole moments for the gravitational wave flux from binary inspirals to third post newtonian order. J Cosmol Astropart Phys 3:009
273. Galley CR, Leibovich AK, Rothstein IZ (2010) Finite size corrections to the radiation reaction force in classical electrodynamics. Phys Rev Lett 105:094802
274. Yolcu C, Rothstein IZ, Deserno M (2011) Effective field theory approach to Casimir interactions on soft matter surfaces. Europhys Lett 96:20003
275. Yolcu C, Rothstein IZ, Deserno M (2012) Effective field theory approach to fluctuation induced forces between colloids at an interface. Phys Rev E 85:011140

276. Dommersnes PG, Fournier JB (1999) Casimir and mean field interactions between membrane inclusions subject to external torques. Europhys Lett 46:256
277. Kardar M, Golestanian R (1999) The "friction" of vacuum, and other fluctuation induced forces. Rev Mod Phys 71:1233–1245
278. Park J M, Lubensky TC (1996) Interactions between membrane inclusions on fluctuating membranes. J Phys I France 6(9):1217–1235
279. Helfrich W, Weikl TR (2001) Two direct methods to calculate fluctuation forces between rigid objects embedded in fluid membranes. Eur Phys J E 5:423–439
280. Gosselin HP, Morbach H, Müller MM (2012) Interface mediated interactions: entropic forces of curved membranes. Phys Rev E 83:051921
281. Brakke KA (1992) The surface evolver. Exp Math 1:141–165
282. Reynwar BJ, Illya G, Harmandaris VA, Müller MM, Kremer K, Deserno M (2007) Aggregation and vesiculation of membrane proteins by curvature mediated interactions. Nature 447:461–464
283. Kim KS, Neu J, Oster G (1998) Curvature mediated interactions between membrane proteins. Biophys J 75(5):2274–2291
284. Kim KS, Neu JC, Oster GF (1999) Many body forces between membrane inclusions: a new pattern formation mechanism. Europhys Lett 48(1):99–105
285. Kim KS, Chou T, Rudnick J (2008) Degenerate ground state lattices of membrane inclusions. Phys Rev E 78:011401. doi:10.1103/PhysRevE.78.011401
286. Müller MM, Deserno M (2010) Cell model approach to membrane mediated protein interactions. Progr Theor Phys Suppl 184:351–363
287. Auth T, Gompper G (2009) Budding and vesiculation induced by conical membrane inclusions. Phys Rev E 80:031901. doi:10.1103/PhysRevE.80.031901
288. Johnson ME, Head Gordon T, Louis AA (2007) Representability problems for coarse grained water potentials. J Chem Phys 126(14):144509
289. Nielsen SO, Lopez CF, Srinivas G, Klein ML (2003) A coarse grain model for n alkanes parameterized from surface tension data. J Chem Phys 119:7043–7049
290. Mognetti BM, Yelash L, Virnau P, Paul W, Binder K, Müller M, Macdowell LG (2008) Efficient prediction of thermodynamic properties of quadrupolar fluids from simulation of a coarse grained model: the case of carbon dioxide. J Chem Phys 128:104501
291. DeVane R, Shinoda W, Moore PB, Klein ML (2009) Transferable coarse grain nonbonded interaction model for amino acids. J Chem Theory Comput 5:2115–2124
292. Tschöp W, Kremer K, Batoulis J, Burger T, Hahn O (1998) Simulation of polymer melts. I. coarse graining procedure for polycarbonates. Acta Polym 49(2–3):61–74
293. Lyubartsev AP, Laaksonen A (1995) Calculation of effective interaction potentials from radial distribution functions – a reverse Monte Carlo approach. Phys Rev E 52:3730–3737
294. Reith D, Putz M, Müller Plathe F (2003) Deriving effective mesoscale potentials from atomistic simulations. J Comp Chem 24:1624–1636
295. Peter C, Delle Site L, Kremer K (2008) Classical simulations from the atomistic to the mesoscale: coarse graining an azobenzene liquid crystal. Soft Matter 4:859–869
296. Murtola T, Karttunen M, Vattulainen I (2009) Systematic coarse graining from structure using internal states: application to phospholipid/cholesterol bilayer. J Chem Phys 131:055101
297. Lyubartsev A, Mirzoev A, Chen LJ, Laaksonen A (2010) Systematic coarse graining of molecular models by the Newton inversion method. Faraday Discuss 144:43–56
298. Savelyev A, Papoian GA (2009) Molecular renormalization group coarse graining of electrolyte solutions: application to aqueous NaCl and KCl. J Phys Chem B 113:7785–7793
299. Megariotis G, Vyrkou A, Leygue A, Theodorou DN (2011) Systematic coarse graining of 4 cyano 4′ pentylbiphenyl. Ind Eng Chem Res 50:546–556
300. Mukherjee B, Site LD, Kremer K, Peter C (2012) Derivation of a coarse grained model for multiscale simulation of liquid crystalline phase transitions. J Phys Chem B 116:8474–8484

301. Shell MS (2008) The relative entropy is fundamental to multiscale and inverse thermo dynamic problems. J Chem Phys 129:144108
302. Silbermann JR, Klapp SHL, Schoen M, Chennamsetty N, Bock H, Gubbins KE (2006) Mesoscale modeling of complex binary fluid mixtures: towards an atomistic foundation of effective potentials. J Chem Phys 124:074105
303. Allen EC, Rutledge GC (2009) Evaluating the transferability of coarse grained, density dependent implicit solvent models to mixtures and chains. J Chem Phys 130:034904
304. Mullinax JW, Noid WG (2009) Extended ensemble approach for deriving transferable coarse grained potentials. J Chem Phys 131:104110
305. Villa A, Peter C, van der Vegt NFA (2010) Transferability of nonbonded interaction potentials for coarse grained simulations: benzene in water. J Chem Theory Comput 6:2434 2444
306. Izvekov S, Chung PW, Rice BM (2010) The multiscale coarse graining method: assessing its accuracy and introducing density dependent coarse grain potentials. J Chem Phys 133:064109
307. Shen JW, Li C, van der Vegt NFA, Peter C (2011) Transferability of coarse grained potentials: implicit solvent models for hydrated ions. J Chem Theory Comput 7:1916 1927
308. Brini E, Marcon V, van der Vegt NFA (2011) Conditional reversible work method for molecular coarse graining applications. Phys Chem Chem Phys 13(10):468 10474
309. Liu Z, Yan H, Wang K, Kuang T, Zhang J, Gul L, An X, Chang W (2004) Crystal structure of spinach major light harvesting complex at 2.72 Å resolution. Nature 428:287 292
310. Standfuss R, van Scheltinga ACT, Lamborghini M, Kühlbrandt W (2005) Mechanisms of photoprotection and nonphotochemical quenching in pea light harvesting complex at 2.5 Å resolution. EMBO J 24:919 928
311. Schmid VH (2008) Light harvesting complexes of vascular plants. Cell Mol Life Sci 65(22): 3619 3639
312. Yang C, Horn R, Paulsen H (2003) The light harvesting chlorophyll a/b complex can be reconstituted in vitro from its completely unfolded apoprotein. Biochemistry 42:4527 4533
313. Horn R, Grundmann G, Paulsen H (2007) Consecutive binding of chlorophylls a and b during the assembly in vitro of light harvesting chlorophyll a/b protein (LHCIIb). J Mol Biol 366:1045 1054
314. Dockter C, Volkov A, Bauer C, Polyhach Y, Joly Lopez Z, Jeschke G, Paulsen H (2009) Refolding of the integral membrane protein light harvesting complex II monitored by pulse EPR. Proc Natl Acad Sci USA 106(44):18485 18490
315. Horn R, Paulsen H (2004) Early steps in the assembly of light harvesting chlorophyll a/b complex. J Biol Chem 279(43):44400 44406
316. Dockter C, Müller AH, Dietz C, Volkov A, Polyhach Y, Jeschke G, Paulsen H (2012) Rigid core and flexible terminus: structure of solubilized light harvesting chlorophyll a/b complex (LHCII) measured by EPR. J Biol Chem 287:2915 2925. doi:10.1074/jbc.M111.307728
317. Garab G, Lohner K, Laggner P, Farkas T (2000) Self regulation of the lipid content of membranes by non bilayer lipids: a hypothesis. Trends Plant Sci 5(11):489 494